

Uyen Truong

# Voxer: Reducing Energy Dissipation of Internal Fluid Flow

Comparative testing of Voxer on water cooling piping system at Keravan Energy

Helsinki Metropolia University of Applied Sciences

Bachelor of Engineering

Environmental Engineering

Thesis

21.5.2018

Author(s) Title	Uyen Truong Voxer: Reducing Energy Dissipation of Internal Fluid Flow
Number of Pages Date	34 pages + 5 appendices 21 May 2018
Degree	Bachelor of Engineering
Degree Programme	Environmental Engineering
Professional Major	Water Resource Management
Instructor(s)	Kaj Lindedahl, Principal Lecturer, Metropolia UAS Prof. Juhani Pylkkänen, Chief Engineer, SansOx Ltd
<p>Reducing energy dissipation inside a tube in fluid process engineering is one of the key factors to improve the efficiency of an industrial process. The purpose of this project is to demonstrate the ability to reduce fluid energy dissipation by utilizing a half elliptical blade wing named Voxer from SansOx Limited (SansOx Ltd.) inside a pipeline. The project was carried out by performing comparative testing on replication models of pipeline section belonging to water cooling system at Keravan Energy's biomass power plant. The Voxer inherits features from static mixer to create vortex current and has innovative characteristics to act as a cost-effective add-on solution for existing pipeline systems.</p> <p>Fluid Flow experimentation on Voxer by measuring pressure drop shows that with the correct position of Voxer in the system, raising of vortex flow reduces pressure drop, which is proportional with decreasing energy losses in the fluid.</p>	
Keywords	SansOx, vortex, Voxer, internal fluid flow, reduce energy dissipation, reduce turbulence, pressure loss, flow loss

## Acknowledgement

A journey of this thesis project has been exciting and challenging and leaving me so many cravings of further studies for this project. If you happen to read these lines while exploring your next research and thesis topic, please consider its potential in building new theory in hydraulic engineering and fluid dynamic field.

First of all, I would like to thank SansOx Limited for granting us this challenging project. I felt very honored to work with the creator of this innovative invention. Prof. Juhani Pylkkänen, Chief Engineer of SansOx Ltd., has given me and my teammate wonderful guidance and plentiful of resources on the project. I also would like to send my appreciation Mikael Seppälä, the CEO, for offering us a tremendous amount of support and encouraging us to explore all possibilities for this project on our own.

Secondly, I would like to thank my thesis supervisor, Kaj Lindedahl of Metropolia UAS. He gave me a lot of insightful remarks and corrections on our papers. A great gratitude toward Mr. Lindedahl, Tomi Hämmäläinen, a lecturer from Environmental and Energy Engineering Department, and Joel Kontturi, a project engineer from Mechanical Engineering laboratory, for guiding, supervising and providing best facilities for our experiments. I also want to send respects to Eka Tuomainen and all the engineers for their exceptional hospitality and support at Keravan Energy.

Most of all, I wouldn't be able to finish this project without Toni Hämmäläinen, my teammate of this thesis project. Thank you for enduring my limited Finnish language skill and me being a complete novice in practical mechanical engineering.

With a special mention to Yifan Yu, a great friend who introduced me to  $\LaTeX$ , and to all of my friends and family members who provided me supports throughout my whole journey in Finland.

I am honored.

## Contents

1	Introduction	1
2	Theoretical background	2
2.1	Internal flow in circular pipe	2
2.1.1	Reynolds number	2
2.1.2	Laminar flow	3
2.1.3	Turbulent flow	3
2.1.4	Major and Minor Losses	4
2.2	Vortex Flow	5
2.3	Flow Motion in 90° pipe bend	5
3	Subjects of Experiment	6
3.1	Keravan biomass power plant system	6
3.1.1	Overview of Keravan biomass power plant	6
3.1.2	Piping cooling section	7
3.2	Voxer	8
3.2.1	History of mechanical mixer	8
3.2.2	Principle Design	9
3.2.3	Functions	9
3.2.4	Economical value	9
3.2.5	Theory gap from literature review	10
4	Methodology	11
4.1	Measurement parameters	11
4.2	Instruments and equipments	12
4.3	Data collection	12
5	Experimentation	13

5.1	Laboratory experimentation	13
5.1.1	Experiment's design	13
5.1.2	Setting of experiments	15
5.1.3	Result and analysis	17
5.2	Experimentation in Keravan Energy	19
5.2.1	Experiment's design	20
5.2.2	Setting of experiments	21
5.2.3	Result and analysis	22
6	Discussion and Conclusion	28
6.1	Discussion	28
6.2	Limitations and Recommendations	29
6.3	Conclusion	32
	References	33
	Appendices	
	Appendix 1 Data analysis	
	Appendix 2 CAD drawing of piping section used in Keravan Energy	
	Appendix 3 List of components and equipments	
	Appendix 4 Raw data from laboratory test	
	Appendix 5 Raw data from Keravan Energy test	

## Abbreviations

<b>ABS</b>	Acrylonitrile butadiene styrene.
<b>CAD</b>	Computer-Aided Design.
<b>CFD</b>	Computational Fluid Dynamics.
<b>CS</b>	Carbon Steel.
<b>CSV</b>	Comma Separated Values file.
<b>EFD</b>	Experimental Fluid Dynamics.
<b>LLDPE</b>	Linear low-density polyethylene.
<b>PP</b>	Polypropylene.
<b>SansOx Ltd.</b>	SansOx Limited.
<b>SS</b>	Stainless Steel.

## Glossary

<b>cavitation</b>	the formation of vapour cavities in a liquid, small liquid-free zones.
<b>no-slip condition</b>	When the fluid flows next to a solid boundary, the fluids attach to the surface which is equivalent to having no velocity.
<b>viscosity</b>	the resistance of a fluid to a change in shape, or movement of neighbouring portions relative to one another.

## 1 Introduction

Minimizing fluid energy losses is one of the important missions in hydraulic engineering and chemical engineering to improve the overall efficiency of the system. The flow resistance in a pipe is caused by various reasons, such as viscosity, pipe roughness or change of velocity.

The new product from SansOx Ltd. is an economic solution to this problem. The product is called Voxer, which consists of a Voxer wing to be inserted into a tube. The wing creates vortex flow that reduces turbulence and flow losses in the tube. Voxer can be installed in various places allocated accordingly in a whole pipeline.

The objectives of this thesis are to present Voxer's function in reducing energy dissipation in the pipe and to examine the effect of different Voxer wing's combinations. The project was also carried out to analyze the hydraulic phenomenon and determine the commercialized Voxer's performance.

The experiments were conducted in the biomass power plant of Keravan Energy Limited. Keravan Energy Ltd. is a state-owned company in Kerava and Sipoo municipality. The object of this study is the water cooling piping system of the power plant.

SansOx Limited is the commissioner of this project. SansOx Ltd. focuses on researching, developing and marketing fresh innovation solutions for clean water market worldwide. Their goal is to develop products in order to provide the optimal sustainable solutions for customers' needs in water treatment, process wastewater treatment, fish farming and agriculture. By executing this study, we will contribute to a completed theory profile of Voxer with quantitative research regarding hydraulic and geometrical parameters of an industrial piping system.

In this thesis, we will demonstrate the experimental fluid dynamics setup and analysis on Voxer under laboratory condition and realistic condition in the power plant. Also, the limitation and possible further study will be discussed.

## 2 Theoretical background

In this chapter, basic principles and theories in fluid dynamics related to the problem of vortex current inside the pipeline are reviewed. These include theoretical backgrounds of internal flow in a circular pipe, flow motion in a curved pipe and vortex flow, which can be found in Fluid Mechanics textbook, peer-review articles, and journals. After considering theoretical literature review the subject, we identify the gap of related theory on subjects of the experiment.

### 2.1 Internal flow in circular pipe

#### 2.1.1 Reynolds number

Reynolds number is one of the key points to define fluid properties, predict flow patterns in different fluid situations. It is expressed as a ratio of inertial forces and viscous forces in the fluid.

$$Re = \frac{\text{Inertial forces}}{\text{Viscous forces}} = \frac{V_{avg} D}{\nu} = \frac{\rho V_{avg} D}{\mu} \quad (1)$$

$V_{avg}$  is the average flow velocity ( $m/s$ );  $D$  is the diameter of pipe ( $m$ );  $\nu$  or  $\frac{\mu}{\rho}$  is the kinematic viscosity of fluid ( $m^2/s$ ). The transition flow from laminar to turbulent depends on the degree of disturbance of flow by surface roughness, pipe vibrations and fluctuations in upstream flow (p.349) [1]. For Newtonian fluids, Reynolds number is:

$$\begin{array}{ll} Re \leq 2300 & \text{laminar flow} \\ 2300 \leq Re \leq 4000 & \text{transitional flow} \\ Re \geq 4000 & \text{turbulent flow} \end{array}$$



### 2.1.2 Laminar flow

Laminar flow in the pipe has  $Re \leq 2300$  which is smooth and highly ordered motion moving in a straight line parallel to the surface. The flow is fully developed without any disruption if the pipe is sufficiently long enough (p.353) [1]. There are no cross-currents perpendicular to the direction of flow, nor eddies or swirls of fluids. Laminar flow is a flow establishment indicated by high momentum diffusion and low momentum convection. Laminar flow is described as a novel flow which usually occurs under highly controlled condition.

### 2.1.3 Turbulent flow

In our investigation, the flow is turbulent as well as most of the encountered situations. In daily life, it can be seen under a form of waves, storm clouds, fast flowing rivers, etc. Turbulent flow with  $Re \geq 4000$  which is usually chaotic and has rapid fluctuations (p.361) [1]. In turbulent flow, the swirling eddies transport mass, momentum, and energy to other regions of flow much more rapidly than molecular diffusion, greatly enhancing mass, momentum, and heat transfer. Therefore, it usually has higher friction values, heat transfer, and mass transfer coefficients.

Sometimes, there are unstable vortices in many sizes interacting with each other, which increase friction effects leading to drag effect. The drag effect makes the pump needed more energy to pump fluid through the pipe. This also resonates with the pipe or form cavitation that increase energy dissipation. While the velocity profile in laminar flow is parabolic, the velocity profile in turbulent flow develops fuller and has a sharp drop near pipe wall. In the pipe, the thin layer next to the wall is called

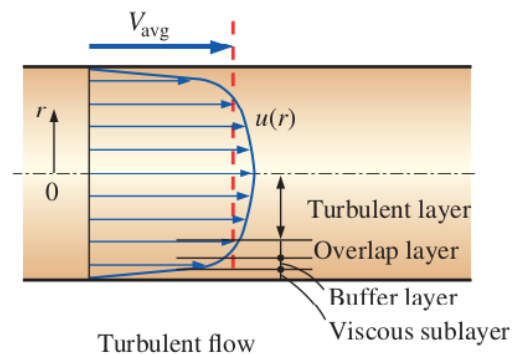


Figure 1: Velocity profile of turbulent flow [1]

viscous sublayer (see figure 1) where viscous effects are major. Next to it is the buffer layer where turbulent effects are getting significant but still affect largely by viscous layer. Above this layer is transition layer, in which the turbulent effects are getting stronger.

### 2.1.4 Major and Minor Losses

In a typical piping system, the fluid goes through various components like fittings, valves, bends, elbows, reducer, etc, in addition to a straight section of piping. Major losses are defined by head loss or pressure loss in straight sections and minor losses occur in the other components of piping.

**Pressure loss** is expressed as:

$$\Delta P_L = f \frac{L}{D} \frac{\rho V_{avg}^2 D}{2} \quad (2)$$

$\frac{\rho V_{avg}^2 D}{2}$  is the dynamic pressure in the pipe;  $f$  is the Darcy- Weisbach friction factor. The equivalent expression for pressure loss is well known as equivalent fluid column height or **head loss**. Head loss represents *the additional height that the fluid needs to be raised by a pump in order to overcome the frictional losses in the pipe* (p.356) [1]. It is obtained by:

$$h_L = \frac{\Delta P_L}{\rho g} = f \frac{L}{D} \frac{V_{avg}^2}{2g} \quad (3)$$

In another hand, minor losses are usually asserted as loss coefficient  $K_L$ . Loss coefficient depends on the geometry of component and the Reynolds number. However, Reynolds number is usually ignored. It is defined as:

$$K_L = \frac{h_L}{v^2/(2g)} \quad (4)$$

In this case,  $h_L$  is an additional irreversible head loss caused by insertion of the component. When loss coefficient is available, **minor head loss** for the component can be also derived from  $L_{equiv}$  as the equivalent length:

$$h_L = K_L \frac{V^2}{2g} = f \frac{L_{equiv}}{D} \frac{V^2}{2g} \quad (5)$$

$$L_{equiv} = \frac{D}{f} K_L \quad (6)$$

The general total head loss in the piping system is determined from:

$$h_{L,total} = h_{L,major} + h_{L,minor} \quad (7)$$

## 2.2 Vortex Flow

Vortex flow, a major component of turbulent flow, is a region of a fluid revolving around an axis line. The fluid flow velocity is strongest close to its axis and reduces in an inverse proportion to the distance of the axis. Vortex is best to describe by vorticity, a rotation vector of the fluid element defined by mathematically by a curl of velocity  $\vec{V}$ . There are two types of the vortex: irrotational vortex and rotational vortex. Rotational vortices happen when the vorticity at a point in the flow field is zero and the fluid particle occupying that point is rotating (p.156) [1]. The fluid itself doesn't generate the vortex rotation but external or extra forces which apply on it to keep the motion going indefinitely. Irrotational vortices are also called free vortices. A vortex evolves fairly quickly toward the irrotational flow pattern, where the flow velocity is inversely proportional to the distance [2]. According to Bernoulli's principle (p.200) [1], the fluid motion in a vortex creates dynamic pressure. This dynamic pressure is lowest in its core region, around the axis, and develops when moving away from it.

## 2.3 Flow Motion in 90° pipe bend

From the knowledge in the section of minor loss, it is said that these losses would occur when going through the curved pipe. In real life condition, the flow motions through the curved pipeline are further than complicated being either laminar, transitional or turbulent and through the presence of swirling or pulsations [3]. When the fluid motion in straight pipe meets the curve, the fluid particle changes their main direction of motion. In the curved conduits, the centrifugal force ( $U^2/R_c$ , where  $U$  is the velocity and  $R_c$  is the radius of curvature) induced from the bend will act stronger on the fluid close to the pipe axis than close to the walls. as the higher velocity fluid is next to the pipe axis. This is an adverse pressure gradient generated from the curvature with an increase in pressure, therefore a decrease in velocity close to the convex wall, and the contrary will occur towards the outer side of the pipe.

### 3 Subjects of Experiment

#### 3.1 Keravan biomass power plant system

##### 3.1.1 Overview of Keravan biomass power plant

Keravan Energy is the main provider of electricity and district heating for the whole Kerava and Sipoo municipality in Southern Finland; they also sell electricity to many parts in Finland as well. Their electricity and district heating are solely produced at Keravan biomass power plant (Keravan bioboimalaitos). [4]

The biomass power plant's production covers about 75% of Kerava city's district heating needs and about 25% of Keravan Energy's electricity purchase. The biomass power plant generates electrical power roughly at the rate of 21 megawatts (*MW*); process heat power generating a capacity of about 10 *MW* and district heating power of about 50 *MW*. The power plant's boiler is fed by domestic fuels from clean wood (branches, barks, chips, twigs, stumps and etc) and milling cuttings. The principle process of the biomass power plant is illustrated in figure 2.

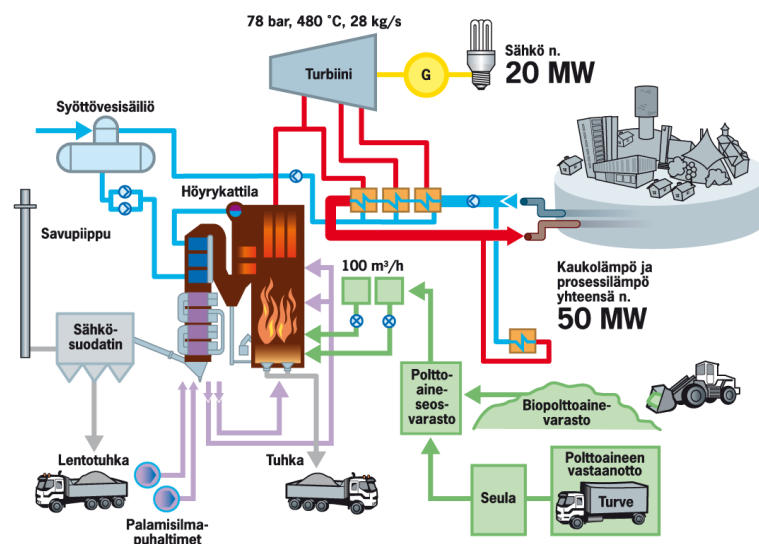


Figure 2: Keravan Energy's biomass power plant working principles chart (Copied from keravanenergia.fi)(2018) [4].

The power plant was built following the principles of Best Available Techniques (BAT) in

2009 [4]. The wood and biomass fuel is received and screened before going into a mixed fuel storage. These mixed wood fuels are fed into a kerosene boiler. In the combustion chamber, the fuels are burned and released combustion gases. These gases go through and heat feed water from feeding water tank. Then they keep going through another cooling system to get into electrostatic precipitator to precipitate fly ash. The exhausted gases from the chimney are already dedusted, damped and desulphurized and safe for the environment. The bottom ash of the boiler is reused in a chamber and collected afterward. Meanwhile, the feed water is transferred into steam in the boiler. The high-pressure steam traveling from the boiler to pipe to drive a turbine. The generator converts kinetic energy from turbine to electricity for the municipality. The remaining heat in the steam is used for district heating. After that, the remaining steam is condensed in a condenser. This condensate in the condenser is fed back to the feed water tank.

### 3.1.2 Piping cooling section

The targeted piping section in our experiment is a part of equipment for ash handling system in Keravan biomass power plant. The cooling system helps to reduce the heat of flying ash in order to help them land down on the surface for ash collection. Figure 3 shows a original piping section that we are going to use for the test.



Figure 3: Targeted piping section altered in the experiment

## 3.2 Voxer

### 3.2.1 History of mechanical mixer

It is said that inspiration for designing Voxer is from the inline motionless mixing industry. The name for the mixer is widely known as a static mixer or motionless mixer. The half elliptical shape of Voxer is partly inspired by the shape of Helical Static Mixer which pioneered in the industry over 45 years [5] and Elliptical Static Mixer (see figure 4).



Figure 4: Elliptical Static Mixer (Copied from [pmiec.com/en/portfolio-items/elliptical-static-mixer/](https://pmiec.com/en/portfolio-items/elliptical-static-mixer/))(2018) [6]

Apparently, mixing is a very common process of industrial process engineering to enhance mixing superior efficiency. There are more than thousands of mechanical mixers developed to maximize fluid mixing and minimize energy consumption by diminishing viscous dissipation effects [7]. Elliptical Static Mixer is suitable for low to medium viscosity fluids, which is usually used in chemical and petroleum industry [6]. The static mixer is a preferable alternative to conventional agitation since it has lower energy dissipations and reduces maintenance need as well as it results in similar or sometimes better performance at a much lower cost. In addition, the static mixer is able to provide homogeneous mixing of feed streams with a minimum residence time [8]. According to Venturi effect, when the cross-sectional internal area is reduced, the flow velocity or flow rate will increase. In the Computational Fluid Dynamics (CFD) simulation of an elliptical static mixer, we can clearly see the separation of original flow leads to the formation of vortex current around center axis of tube (see figure 5 on the following page) to mix combination of fluids homogeneously and the reducing pressure drop along the mixer (see figure 6 on the next page).

The elliptical static mixer can be applied in many different applications like water and waste treatment, gas and liquid mixing, production of biodiesel fuel, injection of a clot on track, viscosity modifier,  $pH$  controller, etc [6].

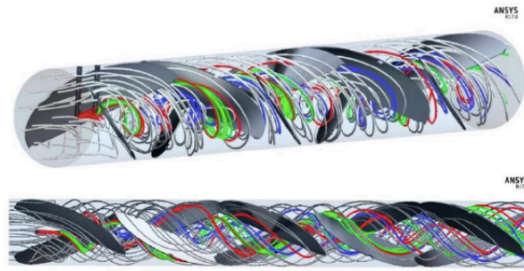


Figure 5: Vortex current created by mixer blades around center axis of tube [9]

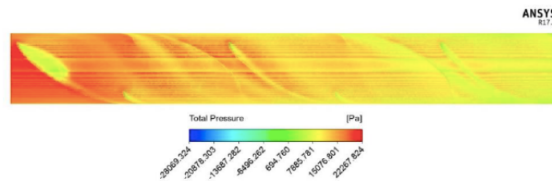


Figure 6: Pressure contour along elliptical static mixer [9]

### 3.2.2 Principle Design

As it is mentioned above, the half-elliptical shape of Voxel is inspired by the semi-elliptical structure of many kinds of the motionless mechanical mixer. Voxel, which includes a vortex flow wing and a tube, was designed by Chief Engineer of SansOx Ltd., Juhani Pylkkänen. Voxel's design is relatively simple. However, more information about the principle design was omitted in this thesis version for confidential reasons.

### 3.2.3 Functions

Mr. Pylkkänen described that the vortex wing of Voxel is going to decrease turbulence and flow losses in a tube, where liquid or gas flows by gravity or pressure [10]. The vortex wing generates vortex flow which smoothens the rotation of mass flow around the tube centerline. Detailed explanation on Voxel wing working principles was extracted out due to confidential issues.

### 3.2.4 Economical value

While the static mixer is more expensive and hard to request customized model for existing pipelines, Voxel is designed in accordance with economical and performance parameters.

Apart from simple design, Voxer can be manufactured with a reasonably cost-effective expense. In addition to cheaper product cost, Voxer is able to deliver many good benefits to customers with lower maintenance and operation cost. With normal screw type of blade, it is needed to be scheduled to be produced during the planning stage of a pipeline system. With Voxer, it can be done easily by self-installation. The flow is smoothly divided into two equal vortex flows flowing in a relation like rolling patterns on their contacts. Without the rolling effect, dirt is formed on cross beam of screw type blades at intake. Apparently, the half ellipse structure installed on the inner tube surface has no cross beam. Hence the blades stay clean and less maintenance is required. This is the best marketable technical feature of the Voxer. Moreover, Voxer has versatile compatibility with various liquids like water, wastewater, slurry, oil and different gases like air, oxygen, nitrogen, natural gas, carbon dioxide and hydrogen [10].

### 3.2.5 Theory gap from literature review

For 40 years, the technology of mechanical mixer has gone through a long way to develop mixing superior efficiency to an advanced level. However, there are still many study gaps in loss reductions of half elliptical structure inside plain tubes, straight and curved pipes. Since homogenous fluids are used any many applications like a pump, water cooling piping, etc, it is necessary to explore the potential in reducing energy dissipation in those applications as well.



## 4 Methodology

There are two aspects of this thesis project. The first aspect is to perform a comparative testing to determine the possibility to commercialize Voxer. The second aspect is to produce materials for supporting theory of Voxer. However, since there is limitation of equipment and software, mainly comparative testing is completed. Data and analysis acquired from the test can be used to support basic theory of Voxer from Experimental Fluid Dynamics (EFD) point of view and to create a database to advance the study further with CFD or with mathematical model later in the future.

Comparative testing is a process of measuring properties of the performance of the product. The primary element which constitutes an objective comparative test program is the extent to which the researchers can perform tests with independence from the manufacturers, suppliers, and marketers of the products [11]. In this project, we performed the comparative testing on Voxer at Keravan Energy for the commissioner SansOx Ltd. in order to provide data for scientific and engineering purposes; subject product to stresses and dynamic expected in use.

### 4.1 Measurement parameters

The measuring device used in both experiments is Danfoss PFM 100, which specializes in measuring differential pressure on both sides of a valve in the hydronic system, which also measures  $K_v$  factor and flow rate [12]. In our measurement, we don't use the valve needle of the measuring device but using a direct insertion of measuring hose into the medium connector to the piping system. The device needs to be calibrated every time before each measurement under static pressure influence. If the fluid circulation isn't closed, there are chances that the fluid is still moving inside pipelines which led to errors in measuring static pressure. Leakages within the system also don't let fluid completely rest, this leads to unstable static pressure calibration.

## 4.2 Instruments and equipments

The experiments focus on reconstructing the structure of the section of piping in the cooling system. The pipeline diameter is categorized as DN50. All of equipments and instruments are mentioned and listed in chapter *Objects of Experiment* and appendix 3.

## 4.3 Data collection

The condition of each comparative measurement presented in the following chapter was attempted to maintain stable data collection. When the data is stable after the flow has completely developed, a pressure change value, the flow rate is recorded into data sheet for each measurement. If the data doesn't achieve stable stage, a video is recorded and values are transcribed into digital data table to plot out the range of values in every measurement. Raw data is listed in appendix 4 and 5.

## 5 Experimentation

In this chapter, we will go through the process, result, and analysis of two experiments for Voxer's comparative testing in Keravan Energy's cooling system. The Computer-Aided Design (CAD) models for pipeline is shown in appendix 2; and source code for analysis are also presented in appendix 1. Figure 3 on page 7 shows the original cooling piping section in Keravan Energy. The pipeline includes these main components: one 5 meters of straight pipe, two 90° elbows and rubber hoses. The pipe used in Keravan Energy is DN50. In these experiments, the fluid flows were recognized as turbulent flow. Turbulent flow occurs when instabilities in a flow are not sufficiently damped by viscous action and the fluid velocity at each point in the flow exhibits random fluctuations [13]. The fluid tested in both of experiment was a Newtonian fluid, water, at moderate temperatures.

### 5.1 Laboratory experimentation

It is essential to get a full understanding of the hydraulic system, product testing, and objectives. In order to achieve this, it is advised to perform comparative measurements under laboratory condition first. In this setting, we will acquire more knowledge about factors which could affect the system, proper techniques, required conditions and practices which needed to be applied to ensure the quality of the measurement. Moreover, the data acquired would be more stable under a controlled setting.

#### 5.1.1 Experiment's design

The main goal of this laboratory experimentation is setting up the closest replication of cooling piping section with Polypropylene (PP) material and determining which Voxer combination is the best for the real test in Keravan Energy.

CAD drawing in figure 7 on the next page illustrates the basic setting of the pipeline. There were 4 measuring points which associated with plane connectors. The reason for

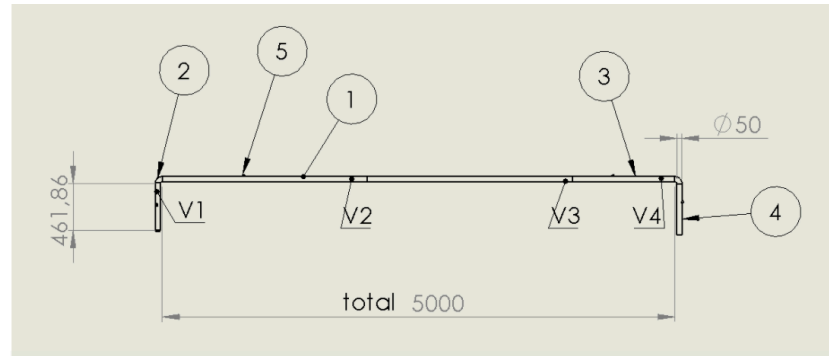


Figure 7: Basic pipe layout and positions of measuring points and Voxel wings  
 1) Straight pipes 2 m; 2) 90° pipe bends; 3) Straight pipe 1 m; 4) Straight pipe 0.5 m; 5) Plane connectors for measuring points

creating these connectors is to create the flat surface for ensuring secured pressurization of measuring points. It also minimized the interference of the measuring device to the pressure and flow in the system. Each Voxel was connected to the end of each straight pipe, except the last one. There were maximum 4 Voxers using in each of measurement. With this setting, the pipeline was divided into 3 sections as pipes in series where total pressure is the accumulation of pressure from each section of the whole pipeline. In this experiment, we named section A from point 1 to 2, section B from point 2 to 3 and section C from point 3 to 4. Section T indicates the whole pipe from point 1 to 4 as the beginning and the end of the system. Since all of the pipes were connected in series, we have:

$$\Delta P_t = P_a + P_b + P_c = P_{ab} + P_c \quad (8)$$

$\Delta P_t$  is the total pressure change in pipeline;  $P_a$ ,  $P_b$  and  $P_c$  are the pressure change in section A, B and C;  $P_{ab}$  is the pressure change in section A and B together.

There were 2 types of Voxel which were used in the test: Voxel 40° DN40 and Voxel 30° DN40. The angle indicates the direction of the outcome flow after going through the Voxel wing. Different combinations of the amount of Voxel and types of Voxel were carried out to determine the behavior of flow in each section and find out the best combination. Table 1 lists out the combinations performed in this test.  $V_1$  was placed before the 1<sup>st</sup> elbow in section A. Section B included  $V_2$  and  $V_3$  at the end of each 2-meter-pipe. The last Voxel  $V_4$  was placed before the ending curved pipe in section C. The mixed combination included 30° Voxel as  $V_1$  and 40° Voxel as  $V_4$ . The pressure changes between section A, section A and B and total pipe were measured in every combination. Every measurement was repeated 10 times to ensure balanced values. During the test, the average tempera-

ture of water in the vessel was measured also to consider its influence on fluid viscosity and surface tension. Measurement for pipe without Voxer installed was performed as well. The inner diameter of the pipe was measured to have Voxer customized as a perfect fit inside the tube. The material of pipes is PP.

Table 1: Voxer combinations in lab test.

Type	V0	V1	V12	V123	V1234	V14
None	X	-	-	-	-	-
30 degree	-	X	X	X	X	X
40 degree	-	X	X	X	X	X
Mixed	-	-	-	-	-	X

### 5.1.2 Setting of experiments

#### Main pipe

The tested pipeline system was set like figure 7 on the preceding page in Metropolia's laboratory. Pipes were connected with others in series. The main straight horizontal pipe section is 5 m long in total, which included two 2 m of straight pipes and one 1 m of straight pipe. Each side of main straight pipe was fitted with a 90° curved pipe. There were two 0.5 m of vertical pipe extensions at each side, acting as extended pipes for placing Voxer and measuring points. Two reducers were attached with these extended in order to accommodate the hose pump. Figure 8 demonstrates the completed setting.



Figure 8: View of the whole test pipeline in Metropolia's lab

### Connectors, pump and vessels

Plastic connectors were 3-D printed. Pressure meter's hoses were attached to the pipe by 4 plastic connectors glued above small holes on the pipe (see figure 9). Voxers were separated from a metal sheet, bent, twisted following given instruction, and inserted into various positions of the pipeline. As mentioned before, the positions of Voxer were mainly at the end of each pipe. The system was set above the ground with 2 vessels at each side to keep the flow going with gravity, one as a water reservoir and one for precaution leaking. A pump was positioned in the water reservoir and connected with the starting pipe by a hose. Water was delivered through the system and come back to the water reservoir. The ending pipe was submerged completely into the water to balance the static pressure in the system (see figure 10). The flow direction was from right to left.



Figure 9: Connector as measuring points



Figure 10: The ending pipe was submerged into water in reservoir

### 5.1.3 Result and analysis

Since the data frame acquired from lab experiment is really extensive, the values from each measurement were aggregated and demonstrated through the following graphs.

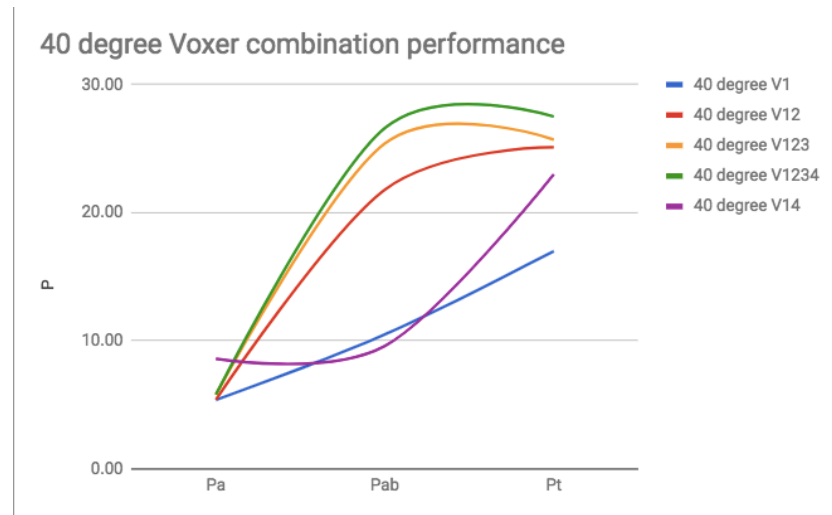


Figure 11: Compare performance of each combination from Voxel 40° DN40

In figure 11, all of the combinations which have Voxel 40° DN40 are compared with each other. When the flow started through the 1<sup>st</sup> Voxel in section A, most of the pressure changes from different combinations result in the similar value around 5 to 7 millibars (*mb*). Section A has the 1<sup>st</sup> Voxel before the curve. This shows that the behavior of flow after each rotation in the pipeline in section A is the same with each other. Starting from section B, we see the drastic change between V1, V14 and the rest of Voxel combinations. The pressure changes between in inflow and before section C are truly dramatic from 7 *mb* to more than 25 *mb* according to combinations with more than 2 Voxers in the pipeline. When comparing pressure of section A and B between combination V1 and V14, V14 is appeared to have less pressure drop than V1. From total pressure drop point of view, V1 has the lowest pressure change while V14 and the rest of combination meet around 24 to 27 *mb*. From this graph, it can be seen that 1 Voxel at position V1 results in the lowest pressure change which means that the pressure loss was reduced.

Figure 12 illustrates the operation of Voxel 30° DN40 from five Voxel combinations. The trendlines from these combinations of Voxel 30° are much more uniform than those trendlines of Voxel 40°. They all started in section A with a short range of pressure change from 5 to 9 *mb*. After section A and B, most of the trendlines except V14 meet each other at the

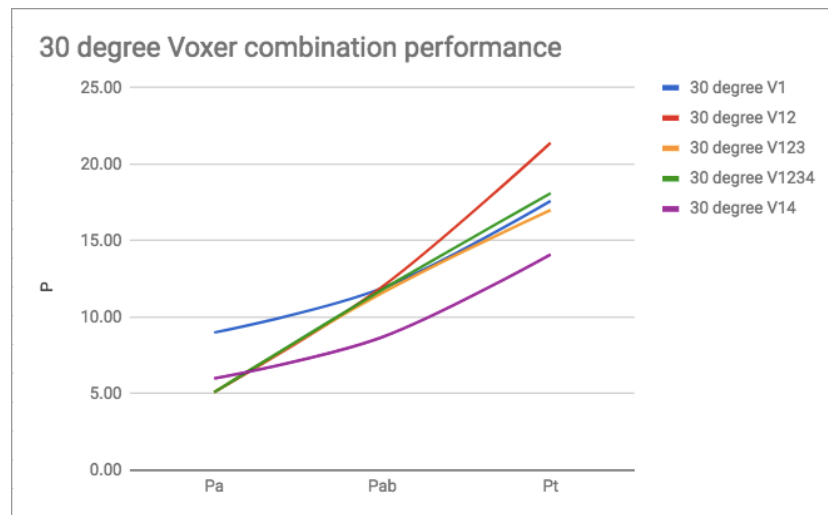


Figure 12: Compare performance of each combination from Voxer 30° DN40

intersection of 12 *mb*. From here, these trendlines don't separate at total pressure (0.5 to 1 *mb* difference) from each other that much except V12 (22 *mb*). Meanwhile, V14 keeps the parallel trendlines at the lower level from 6 to 14 *mb*.

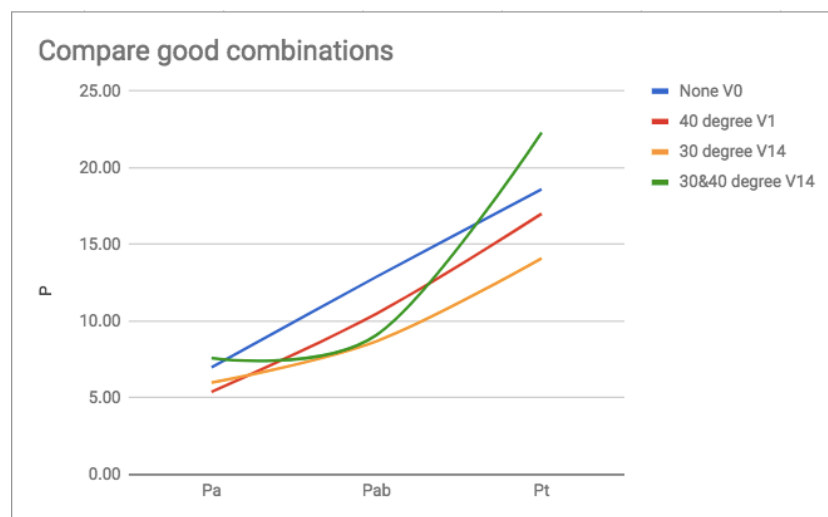


Figure 13: Comparison among good Voxer combinations

We compare the most potent combinations of each Voxer type with the mixed combination and standard pipeline with no Voxer inside in figure 13. It can be clearly seen that the correlation of pressure change along the pipe of the standard pipeline, combination V1 of Voxer 40° and combination V14 of Voxer 30° are almost parallel with each other. The mixed combination V1 (Voxer 30°) and V4 (Voxer 40°) actually reduces sectional pressure loss comparing to original pipe but later it leads to the increase in total pressure change when the flow goes through Voxer 40° at the end of the pipe.



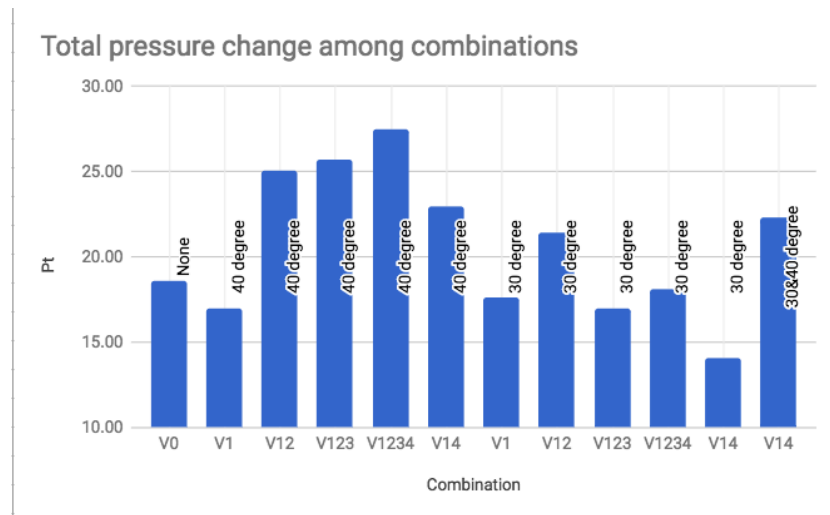


Figure 14: Total pressure change among all combinations

Figure 14 points out those combinations which diminished the flow reduction in the system. Those which reduced the little amount of pressure drop were  $40^\circ - V1$ ,  $30^\circ - V1$ ,  $30^\circ - V123$  and  $30^\circ - V1234$ . It can be concluded that the largest reduction in total pressure is combination  $V14$  of Voxel  $30^\circ DN40$ . In general, Voxel  $30^\circ$  performed better than Voxel  $40^\circ$ . More Voxers in the pipeline, especially inside the main horizontal pipeline would increase pressure change of system in total.

## 5.2 Experimentation in Keravan Energy

With the result of the laboratory test, we used them as the references to the design of alternative pipeline in the cooling system. Information about the system was given from Keravan Energy. It is known that the income flow rate is around  $2\text{ l/s}$  (local measure) at  $1\text{ bar}$  pressure. The input temperature is  $6^\circ\text{C}$  and the output temperature is  $16^\circ\text{C}$ . Since it is not advised to interfere with the existing pipeline of the cooling system, we should assemble an alternative pipeline with characteristics needed for the comparative measurement. In this experiment at Keravan Energy, we observe the behavior of Voxel under realistic uncontrolled condition. The assembly was done in Metropolia's mechanical laboratory.

### 5.2.1 Experiment's design

From the observation of original pipeline section (see figure 3 on page 7, it is clear that Vortex couldn't be placed inside rubber hoses but inside straight steel circular pipe. This also applied to positions of measuring points to measure inflow before the curve and outflow after the pipe bend. The water flow rate in Keravan Energy is much higher than the one from the pump used in the lab test. So there are chances that water would be leaked from the pipe leading to more energy loss. The fact that Vortex wing should be easy to remove from the pipe between different combinations is taken into consideration.

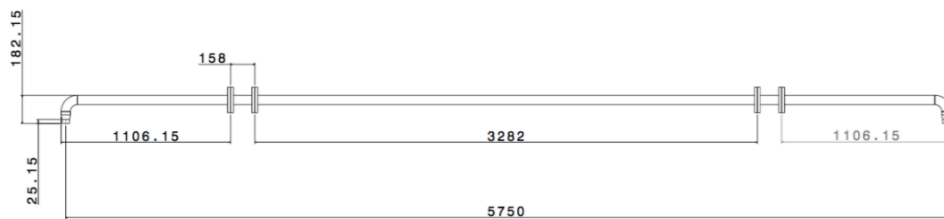


Figure 15: Drawing of pipeline for experiment at Keravan Energy

A design of pipeline shown in figure 15 is the experiment's solution for most of the problems above. The length of pipeline section was taken from CAD documentation of Keravan Energy and measured again at the site. In this setup, there were maximum 2 Vortexes tested in the pipeline. Vortex wings were placed from the separated pipes (we call them Vortex pipes) with flanges which would be easily connected to the main pipe. Rubber hoses were attached to the pipeline by reducers at each side. The measuring points were positioned on the reducers to catch inflow and outflow pressure as well as the middle of the long pipe. We divided this testing pipeline into 2 sections. Section A is from inflow reducer to middle point of the pipe. Section B is from the middle point to the outflow reducer. The same principles were applied to pressure changes of this pipeline:

$$\Delta P_t = P_a + P_b = P_a + P_b \quad (9)$$

In this experiment,  $\Delta P_{ab}$  is the total pressure change in pipeline;  $P_a$  and  $P_b$  are their pressure change in section A and section B. There were two types of Vortex were also tested (Vortex 30° DN50 and Vortex 40° DN50). The first Vortex was positioned in section A and the second one was in the other section. The measurements of the 2<sup>nd</sup> sectional and total pressure were measured by pressure meter. Three combinations of Vortex were measu-

red: None (indicating empty pipe with no Voxer inside), degree 30 (2 Voxers 30° DN50), degree 40 (2 Voxers 40° DN50) (see table 2). The material of pipes is Carbon Steel (CS). All of the components were purchased from Ahnsell and assembled in Metropolia's mechanical lab.

Table 2: Voxer combinations in Keravan Energy's test

Type	V0	V12
None	X	-
30 degree	-	X
40 degree	-	X

## 5.2.2 Setting of experiments

### Components Assembly

#### *Measuring points*

A metal rod was cut into parts and tapped to create a thread for measuring point connectors. Then holes were drilled to create contact spaces with the pressure meter. The cylinder metal parts were welded into reducers and the middle point of long pipe above those holes. Figure 16 on the following page presents the final look of measuring points.

#### *Pipes*

The main 6 m carbon steel pipe was cut into parts: two Voxer pipes, two side pipes, and one long middle pipe. Voxer pipes and long middle pipe were welded with two flanges on each side. Then curves were welded together with side pipes and reducers as a unit. Before welding, the reducers were shaped to fit with the rubber hoses (see figure 17 on the next page).

### Setting up in Keravan Energy

At Keravan Energy, the original pipeline section was removed and altered with our testing pipeline. The frame was raised to hold the weight of the new pipeline with higher height than the original one. New rubber hoses were cut to fit the new pipeline. After testing and adjusting some minor problems in the system, the flow rate was adjusted from 2 to 0.8 l/s

to reduce the pressure applied to minor leaking points along the pipe. Figure 18 shows an overview of the setting.

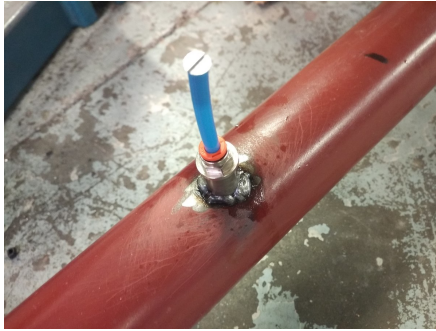


Figure 16: Metal connector as measuring points



Figure 17: Curve, reducer and side pipe



Figure 18: An overview of the testing pipeline

### 5.2.3 Result and analysis

From the observations through the pressure meter, the pressure values of each measurement were not stable and varying in a large range. Apparently with an unfitted framework, the system didn't get really good support so the pipeline resonated axially and radically. The result from Kervan Energy experiment was not as definite as the result of lab experiment since the measurement was performed under an uncontrolled condition in such limited amount of time. Therefore each measurement was recorded in separated videos and transcribed into separate Comma Separated Values file (CSV) files. In the experiment,  $P_b$  and  $P_{ab}$  were recorded. There are 100 points from each measurement transcribed. The flow rate of the system was maintained around  $0.8 \text{ l/s}$  throughout the whole experiment.

There were some minor water leakages around measuring points as well. All of these factors led to pressure value scattering and a significant uncertainty in the result.

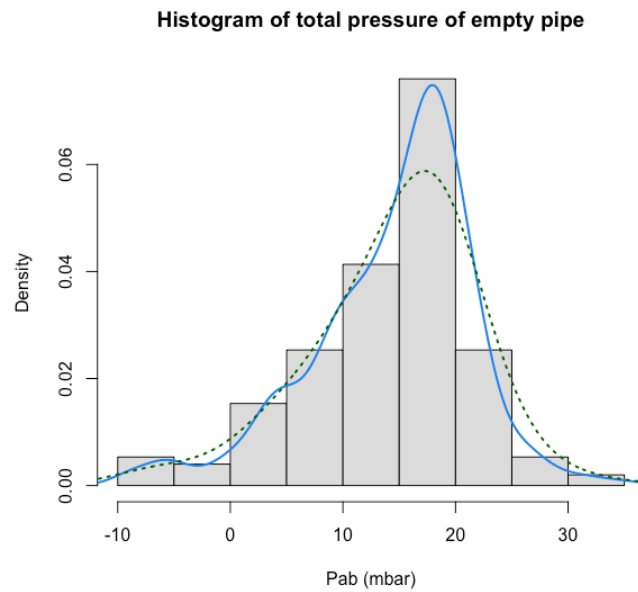


Figure 19: Histogram of total pressure change values in empty pipeline

From Figure 19, it can be seen that the total pressure inside the empty piping section varies in a large range from  $-10$  to  $30$  *mb*. The negative values can be explained as the possibility of cavitation occurrence due to high velocity. The most occurring pressure values are ranged from  $10$  to  $20$  *mb*. The dotted line illustrated smoothed density line of the total pressure in the empty pipe.

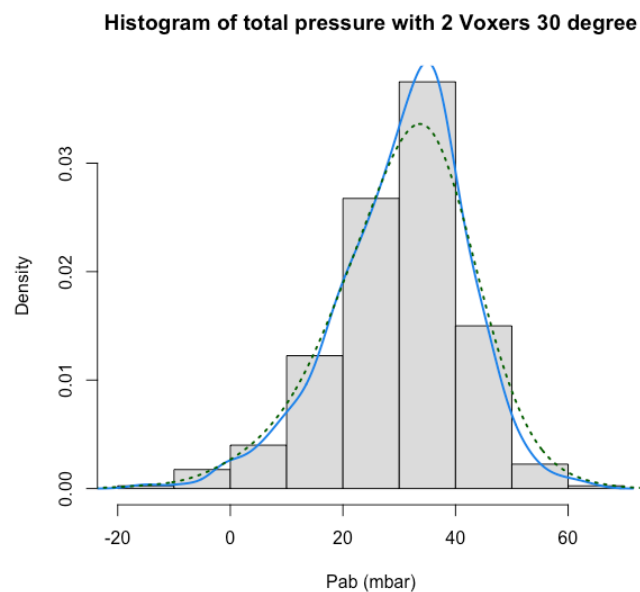


Figure 20: Histogram of total pressure change values with Vortexer  $30^\circ$

It is illustrated in figure 20, the total pressure of a combination of two Voxers 30°. Values range vastly from 0 to 50 *mb*. The most popular values in this combination vary from 20 to 40 *mb*.

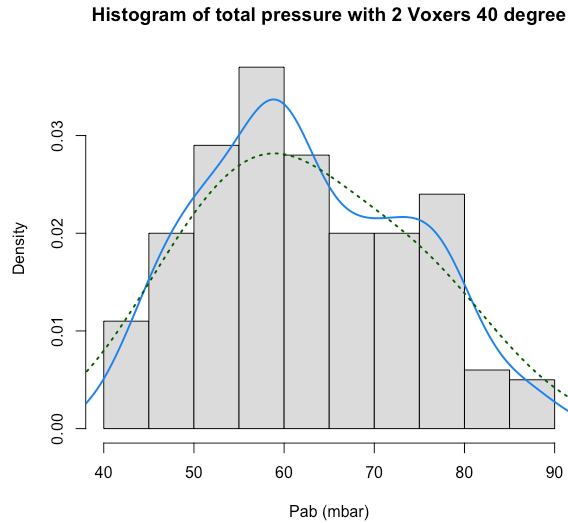


Figure 21: Histogram of total pressure change values with Voxel 40°

There are some differences in combination Voxel 40° with empty pipe and Voxel 30° shown in figure 21. The distribution of two other graphs shows the pattern of normal distribution while this graph shows a large range of value distribution. Values vary from 40 to 90 *mb*, which is much higher than measurements from the empty pipe and Voxel 30°. Pressure change values occur most around 50 to 65 *mb* and from 75 to 80 *mb*.

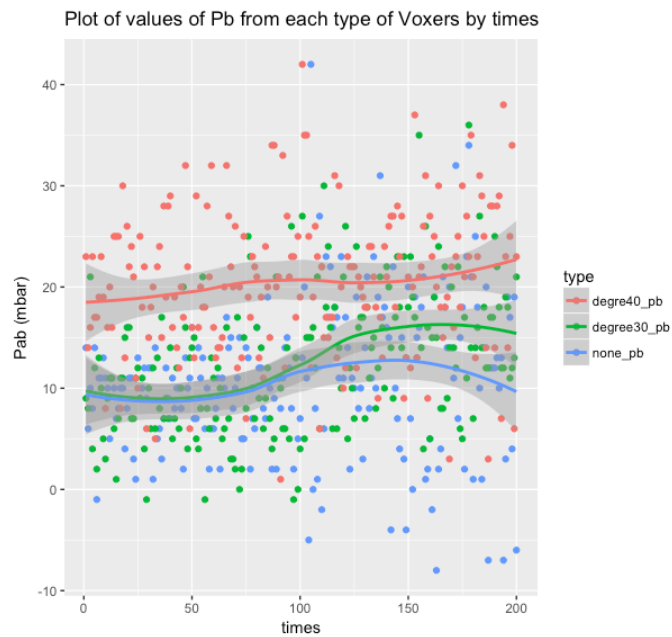


Figure 22: Graph of  $P_b$  among three combinations throughout time

Each point in figure 22 on the previous page represents pressure value of section B with 2<sup>nd</sup> Voxer in the piping section throughout recorded times. The line smoothens the trend of pressure values in each type of combination. From here, we can see that trendline of Voxer 40° is quite constant with pressure changes from 17 to 21 *mb*. Meanwhile, the pressure change's trendlines of empty pipe and Voxer 30° are also aligned with each other.

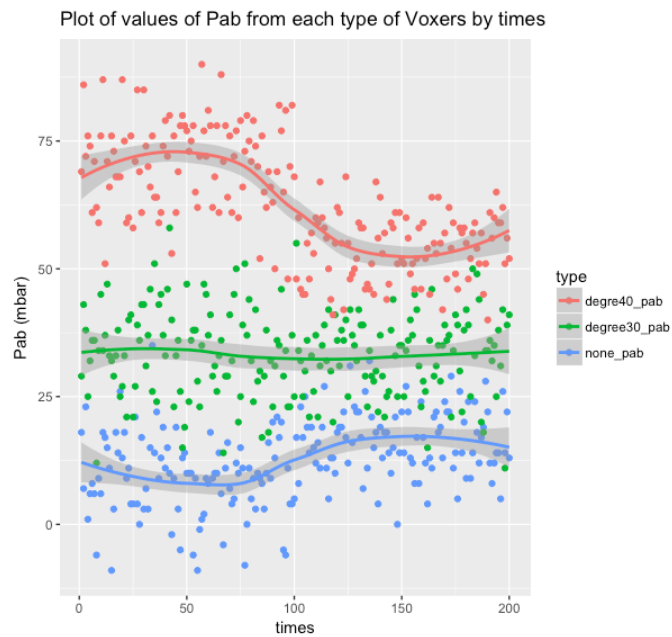


Figure 23: Graph of  $P_{ab}$  among three combinations throughout time

Figure 23 shows the significant division of value range among 3 combinations at total pressure change. Voxer 40° has the largest pressure drop range and reducing pressure drop trendline over time. Empty pipe and Voxer 30° have stable pressure drop over time. Total pressure drop range of Voxer 30° is 20 *mb* larger than the empty pipe.

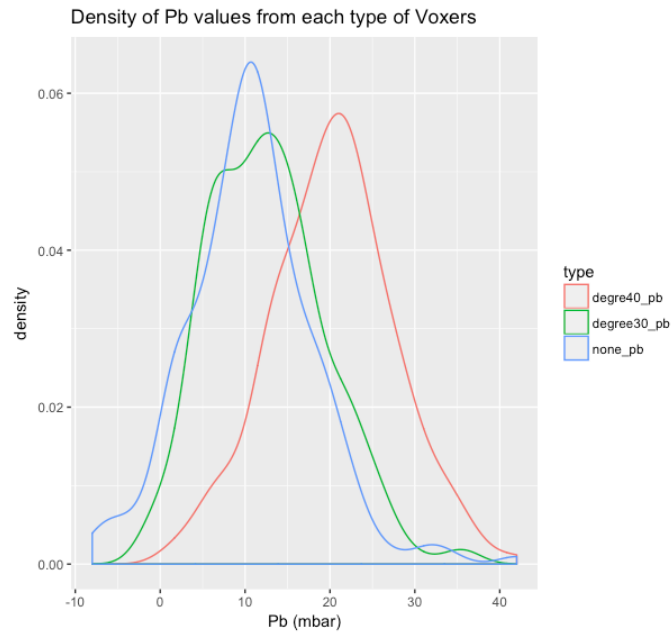


Figure 24: Comparison  $P_b$  values density among three combinations

In the technical document, Mr. Pykkänen mentioned that the optimal position to place the Voxel is where turbulence occurs and flow losses normally. This might be a technically correct statement in section B, where 2<sup>nd</sup> Voxel was placed before the last curve. In figure 24, we see the density of pressure change in section B among 3 combinations. Except for Voxel 40° combination, Voxel 30° presents that it has the potential to reduce pressure drop when compared with empty pipe since it overlaps with the distribution line of empty line with a lower probability.

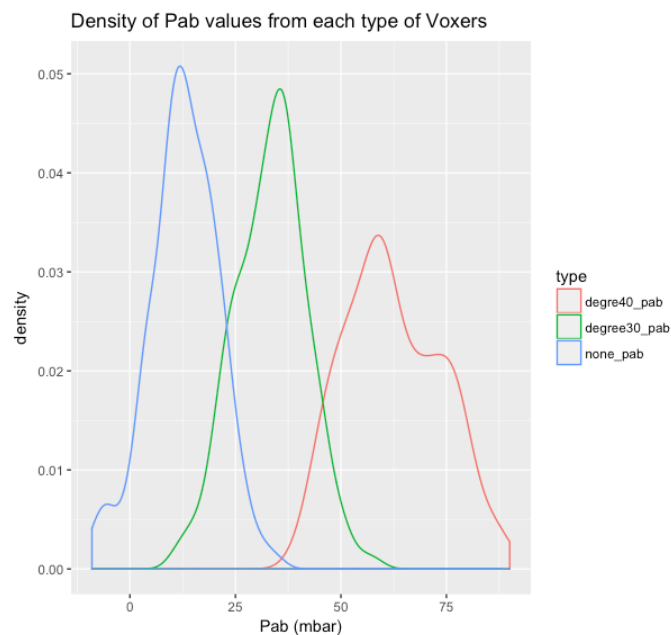


Figure 25: Comparison  $P_{ab}$  values density among three combinations



In the whole pipeline section presented in figure 25, the distribution line of each combination distinctly separates from each other. The distribution line with lowest pressure value is empty, following by Voxer 30° and Voxer 40° is the highest.

## 6 Discussion and Conclusion

In this chapter, the results and analyses from the experiments are deliberated to pull a reasonable explanation for the phenomenon. Limitations and challenges from the experiments are examined as well. After that, some recommendations for the further empirical study on the subject is going to be suggested. Last but not least, a conclusion of the thesis project and possibility to commercialize Voxer are drawn.

### 6.1 Discussion

In the empty pipe, the introduced flow is concentrated around the center region while the flow near the inner wall is affected by no-slip condition. Meanwhile, Voxer disperses the flow to the wall. As observed from the result of both experiments, we can clearly recognize that having Voxer  $40^\circ$  in any position within the pipeline led to a larger rise in pressure losses than Voxer  $30^\circ$ . This could be explained by the dimension difference between two kinds of elliptical shape. The y-axis radius of Voxer  $40^\circ$  is much shorter than Voxer  $30^\circ$  so the vorticity magnitude after Voxer  $40^\circ$  is also shorter.

The shorter vorticity magnitude corresponded to a higher frequency which led to higher pressure [14]. The appearance of Voxer  $40^\circ$  in the mixed combination of 2 types of Voxer showed the impact of shorter vorticity magnitude on pipe pressure.

In the laboratory experiment, the contraction of sectional and total pressure losses by a single Voxer always occurs steadily in the pipelines. It can be said that each Voxer has a nominal resistance and loss reduction. With the presence of many Voxers in series, this can be argued that there was more flow resistance than loss reduction in the piping section. The first Voxer had already resulted in larger loss reduction than resistance but the following Voxers have no loss reduction because the vortex current had already been generated by the first Voxer. With the short distance between each Voxer in those combinations having more than 2 Voxers, the introduced flow wasn't completely developed before meeting the next Voxer. That Voxer became a nuisance to the water flow. Therefo-

re, while its nominal resistance stayed constant, the total and the larger sectional pressure difference is higher.

However, we should also consider the bend at the outflow which caused strong turbulence at the end of the pipeline which might have increased a small amount of total pressure difference in those combinations having only the first Voxer before the starting elbow. The first Voxer reduces energy dissipation in the pipe but the ending curve at the large distance raises pressure drop. That might be a good reason for putting the second Voxer before the ending curve (combination  $V_{14}$  - Voxer  $30^\circ$ ), as recommended in the technical document [10], to support loss reduction in the curved pipe. The performance of this combination was recorded as the best combination in the lab experiment. The reason for this loss reduction in pipe bends is that Voxer creates two separate spiral flow inside the tube. These two spiral flows create the kind of rolling effect in which they roll against each other like roller bearing. This effect leads to the pressure loss reduction in pipe bends.

In Keravan experiment, since the condition was uncontrolled by many minor incidents and outside factors, the evaluation must proceed in a cautious approach to avoid the overconfident conclusion. From all data collected in the experiment, especially the one illustrated in figure 25 on page 26, the difference of total pressure losses among empty pipe, Voxer  $40^\circ$  and Voxer  $30^\circ$  is very distinct. This can be explained by the disproportionation between loss reduction and resistance that was mentioned before. Looking to the sectional pressure change, which is shown in figure 24 on page 26, we can determine that Voxer  $30^\circ$  has a capability to cut down energy dissipations. Since the graph has shown that Voxer  $30^\circ$  has many values which are equal or even lower to values of the sectional pressure loss in the empty pipe. By principle, regarding of vibrations in the pipeline, Voxer wing is also expected to reduce turbulence in the sections of curved pipes, cross fittings, reducers, and valves.

## 6.2 Limitations and Recommendations

There are still many limitations in our study about Voxer which are mainly related to methodology and equipment. In our experiments, we connected the pressure meter to the pipelines by measuring hose attached to a connector which doesn't have direct contact

with the internal flow around the central region. It is doubting that these measuring points are only capable of measuring static pressure but not stagnation pressure. There was the centrifugal force caused by spiral flows which escalated the pressure near the inner tube surface. The original needles [12] attached to measuring hoses might result in better performance in measuring pressure drop. Since this is only a cautious thinking, it would be better to have access to other measuring instruments to compare in order to ensure the better result. In another hand, we could have mitigated the minor leakages problem in Keravan Energy test if we pre-pressurised the piping section before installing directly to the system. With the problem of strong pipe vibrations in a long straight pipe, it is suggested that the vibrations can be partially mitigated by switching vortex angle from  $30^\circ$  to  $40^\circ$  and then switching back to  $30^\circ$ .

Regarding the nominal resistance, Voxel wing's resistance is quite insignificant, as it has neither any cross beam nor any support structures. Because of that, the only flow resistance is Voxel wing's angle which makes vortex flow. In order to lower the resistant level in the pipe, optimizing this angle and tumble finishing sharp edges of the blade should be done beforehand.

There were some time restrictions during both of our experiments which didn't enable us to perform more testings to find out more patterns of the phenomenon and relationships between different variables. They are all crucial points of Voxel wing's functions in any systems. These are some questions suggesting for further researches and testing on Voxel wing:

- *The relationship between Voxers distance and flow profile.* It is assured that if there are more than 2 Voxel wings in this 5 m system, the flow resistance will increase. However, the reason for the variance between different combinations with only 2 Voxers hasn't been resolved yet. How far could the vortex flow travel before it becomes laminar flow? What is the distance between Voxel wings which leads to the optimum flow reduction?
- *The optimal design of Voxel.* Regarding some of the flow losses created by Voxel, the design of Voxel can be pondered to make it more streamlined.

Since the data size from comparative testing was quite restricted and depending on many outside factors, more data from more diverse combinations can be analyzed by building

stimulation model of Voxer in the pipeline by using CFD. Without limitations of time and resources, further research in the future can utilize CFD to perform better stimulation analysis of vortex flow and vibration model by defining correct boundaries corresponding to different structures, fluid properties, model mesh, and related mathematical equations.

There is another important remark on the credibility of the measured parameters in our experiments. According to Bernoulli's principles, the pressure and flow velocity are inversely proportional to each other. In theory, there are a lot of factors which affects to the rise and reduction of pressure drop like the increase of flow speed, the flow resistance or the state of turbulence. In other laboratory tests conducted by SansOx Ltd., it was found that Voxer wing managed to enhance energy efficiency of the system in every measurement, regardless of the amount of Voxer and kinds of angle used in the system. Mass flow over time was measured in their tests instead of pressure drop. There are some uncertainties related to determining energy efficiency or flow losses by surveying pressure drop. Firstly, the speed boost next to the tube surface is the highest increase among other flow regions. Secondly, the impact of the rolling effect from two spiral flows created by Voxer on total pressure hasn't been investigated yet. The third uncertainty is mentioned as the impact of the centrifugal force. The last parameter needs to be considered is the rise of kinetic energy in the spiral vortex flow converted from pressure-based energy. While it contributes more mass flow, it is difficult to convert back to pressure energy when high pressure is needed. This also led the reduction of pressure condition which caused vacuum in the pipe centre which was detected in SansOx Ltd.'s experiments.

### 6.3 Conclusion

Comparative measurements were performed to investigate the effect of Voxer wing of SansOx Ltd. on reducing energy dissipations in the water cooling piping section at Kervan Energy Ltd. The sectional and total pressure difference of the pipelines can be reduced by placing a Voxer  $30^\circ$  before the pipe bend at the end of the piping section. This conclusion is cautiously drawn as it matches the product placement suggestion from the technical document of SansOx Ltd.. In overall, Voxer can be introduced to the market with careful planning for product customization, a lot of trial testings as well as attentive supervision on product placement in customer's system.

## References

- 1 Yunnus A. Çengel and John M. Cimbala. Fluid Mechanics- Fundamentals and Application, Third Edition. New York, the U.S.A.: McGraw Hill. 2014.
- 2 Vortex.. Web document. Wikipedia. <<https://en.wikipedia.org/wiki/Vortex>>. Last checked April 22, 2018.
- 3 Athanasia Kalpakli. Efficiency of the Flow in the Circular Pipe. 2012;.
- 4 Keravan Energia.. Web document. Keravan Energia. <<https://www.keravanenergia.fi/fi/keravan-energia/>>. Last checked April 22, 2018.
- 5 Helical Static Mixer.. Web document. StaMixCo LLC. <<http://www.stamixco-usa.com/helical>>. Last checked April 22, 2018.
- 6 Elliptical Static Mixer.. Web document. Pakzist Modern. <<http://www.pmiac.com/en/portfolio-items/elliptical-static-mixer/>>. Last checked April 22, 2018.
- 7 Fabrizio Sarghini and Annalisa Romano and Paolo Masi. Effect of Different Viscosity on Optimal Shape of Static Mixers for Food Industry. AIDIC Conference Series. 2013;11. <"<http://www.aidic.it/acos/13/11/036.pdf>">.
- 8 Thakur, R. K., Vial, C., Nigam, K. D. P., Nauman, E. B and Djelveh, G. Static mixers in the process industries — a review. Chemical Engineering Research and Design. 2003;81:787–826.
- 9 Moeinoddin Mahmoudi, Reza Goharimehr, Omid Malekhamdi and Ramin Hadi. Designing, analyzing and manufacturing industrial static mixer with DN250 and DN300 in Demin water production unit. 5th International Conference on Science and Engineering. 2016;<"[https://www.researchgate.net/publication/306408924\\_Designing\\_analyzing\\_and\\_manufacturing\\_industrial\\_static\\_mixer\\_with\\_DN250\\_and\\_DN300\\_in\\_Demin\\_water\\_production\\_unit](https://www.researchgate.net/publication/306408924_Designing_analyzing_and_manufacturing_industrial_static_mixer_with_DN250_and_DN300_in_Demin_water_production_unit)">.
- 10 Juhani Pylkkänen. Flow Voxer - Technical Paper. 2016;.
- 11 Mayer, Robert N. . The consumer movement : guardians of the marketplace. Boston: Twayne. 1989.
- 12 PFM 100.. Web document. Danfoss. <<http://products.danfoss.com/productrange/visuals/heatingsolutions/balancing-control-valves/manual-balancing-valves/pfm-100/#/>>. Last checked April 22, 2018.
- 13 Turns S.R. An Introduction to combustion: concept and applications (2nd ed.). 2000;.

- 14 Taewha Park, Yonmo Sung, Taekyung Kim, Inwon Lee, Gyungmin Choi, Duckjool Kim. Effect of static mixer geometry on flow mixing and pressure drop in marine SCR applications. *International Journal of Naval Architecture and Ocean Engineering*. 2014; <"<https://www.sciencedirect.com/science/article/pii/S2092678216302837#bib16>">.



## 1 Data analysis

### 1.1 Mean value of data from laboratory experiment

Type	Delta P	$P_a$	$P_b$	$P_t$
None	V0	7.00	12.90	18.60
40°	V1	5.40	10.50	17.00
	V12	5.40	21.80	25.10
	V123	5.80	25.40	25.70
	V1234	5.80	26.60	27.50
	V14	8.60	9.60	23.00
30°	V1	9.00	11.90	17.60
	V12	5.10	12.00	21.40
	V123	5.10	11.60	17.00
	V1234	5.10	11.80	18.10
	V14	6.00	8.70	14.10
30°- 40°	V14	7.60	9.10	22.30

### 1.2 R code for analysis of Keravan experiment

```

1 library(tidyr)
2 library(ggplot2)
3 # Read data from csv files
4 data = read.csv("Data.csv")
5 for (i in 1:18) {
6   assign(paste("list",i,sep = ""), data[,i])
7 }
8
9 # Create 3 dataframes of each type of Voærs (None, 30 degree, 40 degree)
10 none_data = do.call(rbind, Map(data.frame, Pb = c(list1, list15, list16),
11   Pab = c(list2, list17, list18)))
11 degree30 = do.call(rbind, Map(data.frame, Pb = c(list3, list6, list7,
12   list8), Pab = c(list4,list5, list9, list10)))
12 degree40 = do.call(rbind, Map(data.frame, Pb = c(list12, list13), Pab =
13   c(list11, list14)))
13
14 # Plot histogram and density frequency of total pressure of each type
15 hist(none_data$Pab, main = paste("Histogram of total pressure of empty
16   pipe"), xlab = "Pab (mbar)",probability = TRUE, col = "gray87")
16 lines(density(none_data$Pab), col = "dodgerblue2", lwd =2 )
17 lines(density(none_data$Pab, adjust=2), lty="dotted", col="darkgreen",
18   lwd=2)

```

```

19 hist(degree30$Pab, main = paste("Histogram of total pressure with 2 Voxers
    30 degree"), xlab = "Pab (mbar)",probability = TRUE, col = "gray87")
20 lines(density(degree30$Pab), col = "dodgerblue2", lwd =2 )
21 lines(density(degree30$Pab, adjust=2), lty="dotted", col="darkgreen",
    lwd=2)
22
23 hist(degree40$Pab, main = paste("Histogram of total pressure with 2 Voxers
    40 degree"), xlab = "Pab (mbar)",probability = TRUE, col = "gray87")
24 lines(density(degree40$Pab), col = "dodgerblue2", lwd =2 )
25 lines(density(degree40$Pab, adjust=2), lty="dotted", col="darkgreen",
    lwd=2) # smoothen the line
26
27 # Join Pb values of 3 types of Voxers in a dataframe
28 P_b =do.call(rbind, Map(data.frame,none_pb = c(list15, list16),
    degree30_pb = c(list7, list8),
29     degree40_pb = degree40$Pb))
30 P_b$times = seq.int(nrow(P_b))
31
32 # Join Pab values of 3 types of Voxers in a dataframe
33 P_ab =do.call(rbind,Map(data.frame,none_pab = c(list17, list18),
    degree30_pab = c(list9, list10), degre40_pab = c(degree40$Pab)))
34 P_ab$times = seq.int(nrow(P_ab))
35
36 # Reshape data frame from wide to long
37 rs_Pb = gather(data = P_b, key = "type", value = "Pb", -times)
38 rs_Pab = gather(data = P_ab, key = "type", value = "Pab", -times)
39
40 # Plot lines of Pb and Pab from different groups of Voxers type
41 Pb_plot = ggplot(data = rs_Pb, aes(x = times, y = Pb, colour = type)) +
    geom_point() + geom_smooth()
42 Pb_plot + ggtitle("Plot of values of Pb from each type of Voxers by
    times") + ylab("Pb (mbar)")
43 Pab_plot =ggplot(data = rs_Pab, aes(x = times, y = Pab, colour = type)) +
    geom_point() + geom_smooth()
44 Pab_plot + ggtitle("Plot of values of Pab from each type of Voxers by
    times") + ylab("Pab (mbar)")
45
46 # Compare density line of Pb and Pab from different groups of Voxers type
47 Pb_density = ggplot(data= rs_Pb, aes(Pb, colour = type)) + geom_density()
48 Pb_density + ggtitle("Density of Pb values from each type of Voxers") +
    xlab("Pb (mbar)")
49 Pab_density = ggplot(data= rs_Pab, aes(Pab, colour = type)) +
    geom_density()
50 Pab_density + ggtitle("Density of Pab values from each type of Voxers") +
    xlab("Pab (mbar)")

```

Listing 1: R code

## 2 CAD drawing of piping section used in Keravan Energy

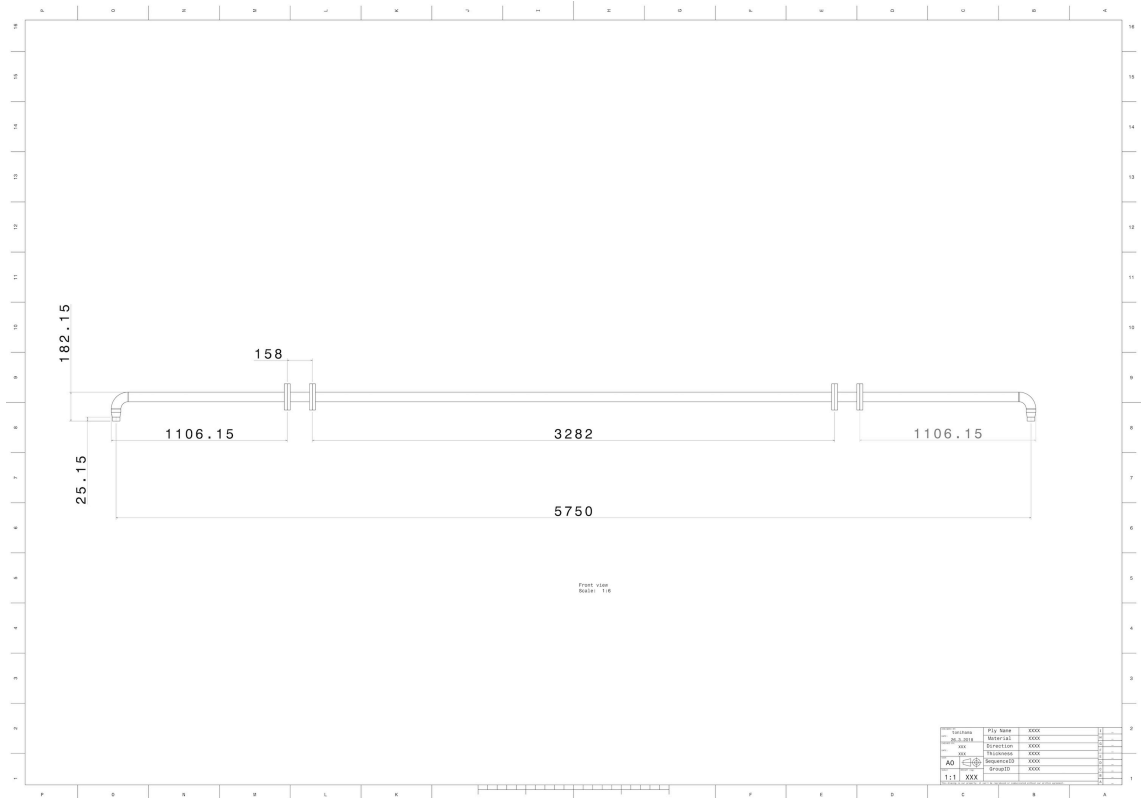


Figure 26: Drawing of whole piping section

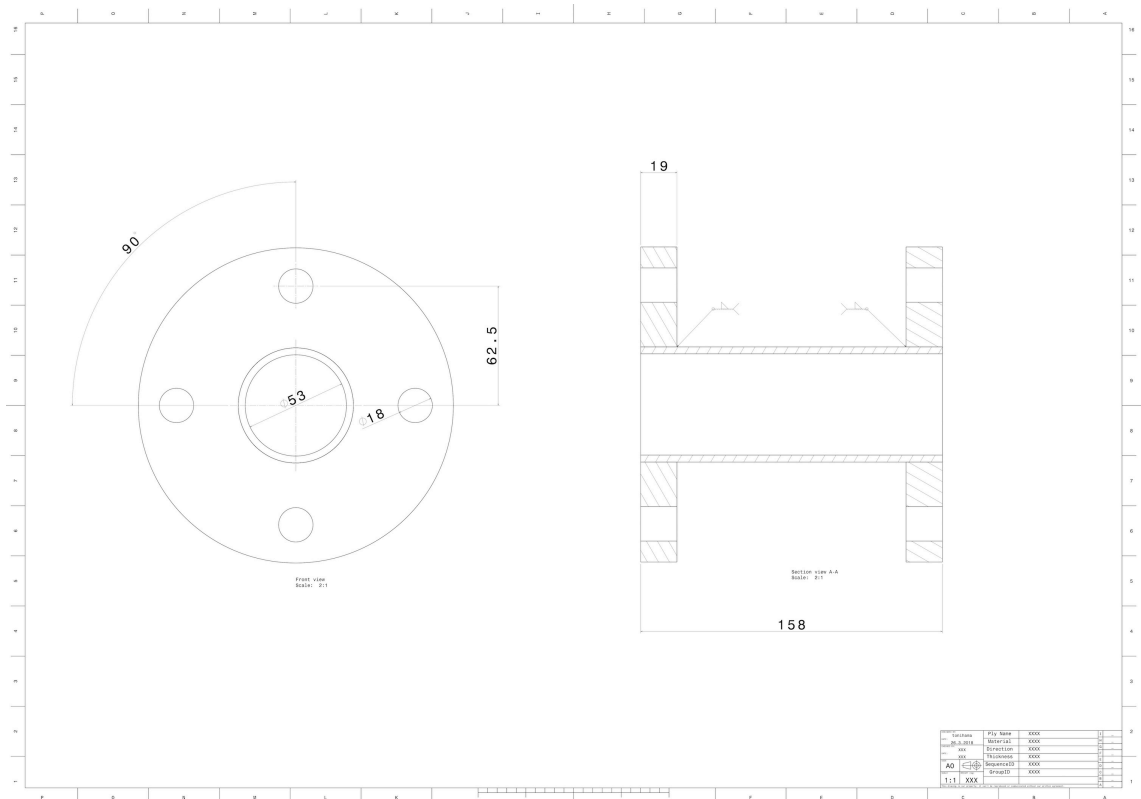


Figure 27: Voxel pipe

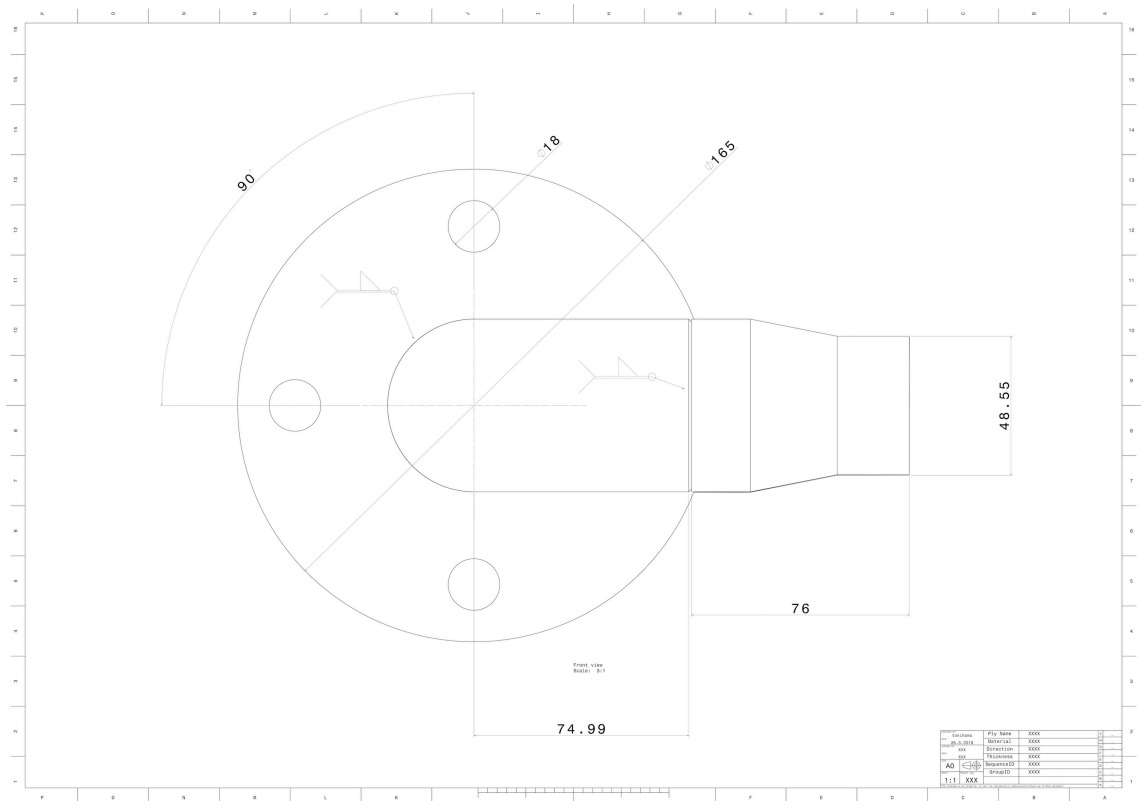


Figure 28: Side view of curved pipe attached to reducer and flange

### 3 List of components and equipments

#### 3.1 Lab test

Materials used are PP, Stainless Steel (SS) and Acrylonitrile butadiene styrene (ABS).

Component	Material	Dimension	Quantity
Straight Pipe	PP	DN50 - ID48 - 2 m	2
Elbow 87°	PP	DN50	2
Straight pipe	PP	DN50 - ID46 - 1 m	1
Straight pipe	PP	DN50 - ID46 - 0.5 m	2
Surface connector	ABS	DN50 - $\varnothing$ 12 - 20 x 20 x 20 mm	4
Pipe connector	PP	DN50	1
Reducer	PP	75 – 50 mm	1
Pump and hose		0.5 l/s	1
Voxer 30°	SS	DN40	4
Voxer 40°	SS	DN40	4
Water vessel			2

#### 3.2 Keravan Energy test

Materials used are CS, SS and Linear low-density polyethylene (LLDPE).

Component	Material	Dimension	Quantity
Reducer	CS	DN50 - 60.3 x 48.3/2.9 mm	2
Straight pipe	CS	DN50 - ID53 - 1062 mm	2
Voxer pipe	CS	DN50 - ID53 - 70 mm	2
Straight pipe	CS	DN50 - ID53 - 3194 mm	1
Elbow 90°	CS	60.3 x 2.9 mm	2
Flange	SS	DN50 - s = 44 mm	8
Bolt	CS	D18	16
Hex nut	CS	D18	16
Washer	CS	D18	32
Voxer 30°	SS	DN50	2
Voxer 40°	SS	DN50	2
Rubber hose	LLDPE		2
Hose clamp	SS		4

#### 4 Raw data from laboratory test

Delta P (mbar)	Flow rate (l/s)	Mean T	Pressure	Voxers	Type
3.00	0.015	19.85	Pa	V0	None
8.00	0.025	19.85	Pa	V0	None
9.00	0.026	19.85	Pa	V0	None
6.00	0.021	19.85	Pa	V0	None
4.00	0.018	19.85	Pa	V0	None
9.00	0.026	19.85	Pa	V0	None
8.00	0.026	19.85	Pa	V0	None
7.00	0.024	19.85	Pa	V0	None
9.00	0.027	19.85	Pa	V0	None
7.00	0.024	19.85	Pa	V0	None
12.00	0.03	19.85	Pab	V0	None
14.00	0.033	19.85	Pab	V0	None
15.00	0.033	19.85	Pab	V0	None
13.00	0.031	19.85	Pab	V0	None
9.00	0.027	19.85	Pab	V0	None
15.00	0.034	19.85	Pab	V0	None
11.00	0.029	19.85	Pab	V0	None
13.00	0.032	19.85	Pab	V0	None
14.00	0.033	19.85	Pab	V0	None
13.00	0.032	19.85	Pab	V0	None
16.00	0.035	19.85	Pt	V0	None
18.00	0.038	19.85	Pt	V0	None
19.00	0.038	19.85	Pt	V0	None
20.00	0.039	19.85	Pt	V0	None
19.00	0.039	19.85	Pt	V0	None
19.00	0.038	19.85	Pt	V0	None
18.00	0.037	19.85	Pt	V0	None
19.00	0.038	19.85	Pt	V0	None
19.00	0.039	19.85	Pt	V0	None
19.00	0.038	19.85	Pt	V0	None
5.00	0.017	16.80	Pa	V1	40 degree
8.00	0.025	16.80	Pa	V1	40 degree
7.00	0.023	16.80	Pa	V1	40 degree
6.00	0.022	16.80	Pa	V1	40 degree
5.00	0.02	16.80	Pa	V1	40 degree
6.00	0.021	15.70	Pa	V1	40 degree
3.00	0.015	17.85	Pa	V1	40 degree
4.00	0.017	17.50	Pa	V1	40 degree
5.00	0.019	17.15	Pa	V1	40 degree
5.00	0.02	16.95	Pa	V1	40 degree

Delta P (mbar)	Flow rate (l/s)	Mean T	Pressure	Voxers	Type
10.00	0.028	17.05	Pab	V1	40 degree
10.00	0.028	16.85	Pab	V1	40 degree
9.00	0.027	16.80	Pab	V1	40 degree
11.00	0.029	16.75	Pab	V1	40 degree
11.00	0.029	16.70	Pab	V1	40 degree
11.00	0.029	16.90	Pab	V1	40 degree
11.00	0.029	16.90	Pab	V1	40 degree
11.00	0.029	17.30	Pab	V1	40 degree
10.00	0.028	17.35	Pab	V1	40 degree
11.00	0.029	17.25	Pab	V1	40 degree
16.00	0.035	17.25	Pt	V1	40 degree
17.00	0.036	17.65	Pt	V1	40 degree
18.00	0.037	17.45	Pt	V1	40 degree
17.00	0.036	17.50	Pt	V1	40 degree
17.00	0.036	17.50	Pt	V1	40 degree
17.00	0.036	17.40	Pt	V1	40 degree
17.00	0.036	17.50	Pt	V1	40 degree
17.00	0.036	17.90	Pt	V1	40 degree
17.00	0.036	17.80	Pt	V1	40 degree
17.00	0.036	17.95	Pt	V1	40 degree
6.00	0.022	17.50	Pa	V12	40 degree
5.00	0.019	17.45	Pa	V12	40 degree
5.00	0.02	17.60	Pa	V12	40 degree
5.00	0.02	17.45	Pa	V12	40 degree
5.00	0.019	17.75	Pa	V12	40 degree
6.00	0.021	18.10	Pa	V12	40 degree
5.00	0.019	18.05	Pa	V12	40 degree
7.00	0.023	18.05	Pa	V12	40 degree
5.00	0.02	17.55	Pa	V12	40 degree
5.00	0.019	17.60	Pa	V12	40 degree
18.00	0.037	17.35	Pab	V12	40 degree
16.00	0.035	17.35	Pab	V12	40 degree
21.00	0.041	17.35	Pab	V12	40 degree
22.00	0.042	18.00	Pab	V12	40 degree
23.00	0.042	18.00	Pab	V12	40 degree
24.00	0.043	18.00	Pab	V12	40 degree
23.00	0.042	18.00	Pab	V12	40 degree
24.00	0.043	18.00	Pab	V12	40 degree
24.00	0.043	18.00	Pab	V12	40 degree
24.00	0.043	18.00	Pab	V12	40 degree
23.00	0.042	18.00	Pab	V12	40 degree

Delta P (mbar)	Flow rate (l/s)	Mean T	Pressure	Voxers	Type
22.00	0.041	19.00	Pt	V12	40 degree
26.00	0.045	19.00	Pt	V12	40 degree
26.00	0.045	19.00	Pt	V12	40 degree
26.00	0.045	19.15	Pt	V12	40 degree
26.00	0.045	17.90	Pt	V12	40 degree
25.00	0.044	17.90	Pt	V12	40 degree
25.00	0.044	17.90	Pt	V12	40 degree
25.00	0.044	17.90	Pt	V12	40 degree
25.00	0.044	17.90	Pt	V12	40 degree
25.00	0.044	17.90	Pt	V12	40 degree
8.00	0.025	18.35	Pa	V123	40 degree
6.00	0.022	18.45	Pa	V123	40 degree
5.00	0.02	18.45	Pa	V123	40 degree
6.00	0.022	18.45	Pa	V123	40 degree
5.00	0.02	18.45	Pa	V123	40 degree
5.00	0.02	18.45	Pa	V123	40 degree
6.00	0.022	18.45	Pa	V123	40 degree
6.00	0.022	18.45	Pa	V123	40 degree
6.00	0.022	18.45	Pa	V123	40 degree
5.00	0.02	18.45	Pa	V123	40 degree
19.00	0.038	19.05	Pab	V123	40 degree
25.00	0.044	19.05	Pab	V123	40 degree
27.00	0.045	19.05	Pab	V123	40 degree
25.00	0.044	19.05	Pab	V123	40 degree
27.00	0.045	19.05	Pab	V123	40 degree
26.00	0.045	19.05	Pab	V123	40 degree
26.00	0.045	19.05	Pab	V123	40 degree
26.00	0.045	19.05	Pab	V123	40 degree
26.00	0.045	19.05	Pab	V123	40 degree
27.00	0.046	19.05	Pab	V123	40 degree
23.00	0.042	18.80	Pt	V123	40 degree
25.00	0.044	18.80	Pt	V123	40 degree
26.00	0.045	18.80	Pt	V123	40 degree
26.00	0.045	18.80	Pt	V123	40 degree
26.00	0.045	18.80	Pt	V123	40 degree
26.00	0.045	18.80	Pt	V123	40 degree
27.00	0.046	18.00	Pt	V123	40 degree
27.00	0.046	18.00	Pt	V123	40 degree
25.00	0.044	18.00	Pt	V123	40 degree
26.00	0.045	18.00	Pt	V123	40 degree



Delta P (mbar)	Flow rate (l/s)	Mean T	Pressure	Voxers	Type
8.00	0.025	18.50	Pa	V1234	40 degree
6.00	0.022	18.50	Pa	V1234	40 degree
5.00	0.02	18.50	Pa	V1234	40 degree
6.00	0.022	18.50	Pa	V1234	40 degree
5.00	0.02	18.50	Pa	V1234	40 degree
5.00	0.02	18.50	Pa	V1234	40 degree
6.00	0.022	18.50	Pa	V1234	40 degree
6.00	0.022	18.50	Pa	V1234	40 degree
6.00	0.022	18.50	Pa	V1234	40 degree
5.00	0.02	18.50	Pa	V1234	40 degree
26.00	0.045	18.50	Pab	V1234	40 degree
27.00	0.046	18.50	Pab	V1234	40 degree
27.00	0.046	18.50	Pab	V1234	40 degree
26.00	0.045	18.50	Pab	V1234	40 degree
26.00	0.045	18.50	Pab	V1234	40 degree
27.00	0.046	18.50	Pab	V1234	40 degree
26.00	0.045	18.50	Pab	V1234	40 degree
27.00	0.046	18.50	Pab	V1234	40 degree
27.00	0.046	18.50	Pab	V1234	40 degree
27.00	0.046	18.50	Pab	V1234	40 degree
27.00	0.046	18.50	Pab	V1234	40 degree
28.00	0.046	18.50	Pt	V1234	40 degree
27.00	0.046	18.50	Pt	V1234	40 degree
28.00	0.047	18.50	Pt	V1234	40 degree
27.00	0.046	18.50	Pt	V1234	40 degree
28.00	0.046	18.50	Pt	V1234	40 degree
27.00	0.046	18.50	Pt	V1234	40 degree
27.00	0.046	18.50	Pt	V1234	40 degree
28.00	0.046	18.50	Pt	V1234	40 degree
28.00	0.046	18.50	Pt	V1234	40 degree
27.00	0.046	18.50	Pt	V1234	40 degree
6.00	0.021	17.35	Pa	V1	30 degree
8.00	0.024	17.35	Pa	V1	30 degree
8.00	0.026	17.35	Pa	V1	30 degree
4.00	0.017	17.35	Pa	V1	30 degree
7.00	0.023	17.35	Pa	V1	30 degree
13.00	0.032	17.50	Pa	V1	30 degree
12.00	0.03	17.50	Pa	V1	30 degree
10.00	0.028	17.50	Pa	V1	30 degree
10.00	0.028	17.50	Pa	V1	30 degree
12.00	0.03	17.50	Pa	V1	30 degree

Delta P (mbar)	Flow rate (l/s)	Mean T	Pressure	Voxers	Type
10.00	0.028	17.50	Pab	V1	30 degree
11.00	0.029	17.50	Pab	V1	30 degree
9.00	0.027	18.00	Pab	V1	30 degree
10.00	0.028	18.00	Pab	V1	30 degree
12.00	0.03	18.00	Pab	V1	30 degree
13.00	0.031	18.00	Pab	V1	30 degree
12.00	0.03	18.00	Pab	V1	30 degree
14.00	0.033	18.00	Pab	V1	30 degree
15.00	0.035	18.00	Pab	V1	30 degree
13.00	0.032	18.00	Pab	V1	30 degree
23.00	0.043	18.00	Pt	V1	30 degree
18.00	0.038	18.00	Pt	V1	30 degree
17.00	0.036	18.00	Pt	V1	30 degree
17.00	0.036	18.20	Pt	V1	30 degree
17.00	0.036	18.20	Pt	V1	30 degree
18.00	0.037	18.20	Pt	V1	30 degree
18.00	0.038	18.20	Pt	V1	30 degree
17.00	0.036	18.20	Pt	V1	30 degree
16.00	0.035	18.20	Pt	V1	30 degree
15.00	0.034	18.20	Pt	V1	30 degree
4.00	0.018	19.05	Pa	V12	30 degree
4.00	0.018	19.05	Pa	V12	30 degree
5.00	0.019	19.05	Pa	V12	30 degree
4.00	0.018	19.05	Pa	V12	30 degree
5.00	0.019	19.05	Pa	V12	30 degree
5.00	0.019	19.05	Pa	V12	30 degree
5.00	0.019	19.05	Pa	V12	30 degree
5.00	0.019	19.05	Pa	V12	30 degree
6.00	0.022	19.05	Pa	V12	30 degree
6.00	0.022	19.05	Pa	V12	30 degree
7.00	0.024	19.05	Pa	V12	30 degree
13.00	0.031	19.05	Pab	V12	30 degree
15.00	0.033	19.05	Pab	V12	30 degree
13.00	0.031	19.05	Pab	V12	30 degree
14.00	0.033	19.05	Pab	V12	30 degree
12.00	0.031	19.05	Pab	V12	30 degree
9.00	0.027	19.05	Pab	V12	30 degree
10.00	0.028	19.05	Pab	V12	30 degree
10.00	0.028	19.05	Pab	V12	30 degree
11.00	0.029	19.05	Pab	V12	30 degree
13.00	0.031	19.05	Pab	V12	30 degree



Delta P (mbar)	Flow rate (l/s)	Mean T	Pressure	Voxers	Type
4.00	0.018	19.50	Pa	V1234	30 degree
4.00	0.018	19.50	Pa	V1234	30 degree
5.00	0.019	19.50	Pa	V1234	30 degree
4.00	0.018	19.50	Pa	V1234	30 degree
5.00	0.019	19.50	Pa	V1234	30 degree
5.00	0.019	19.50	Pa	V1234	30 degree
5.00	0.019	19.50	Pa	V1234	30 degree
6.00	0.022	19.50	Pa	V1234	30 degree
6.00	0.022	19.50	Pa	V1234	30 degree
7.00	0.024	19.50	Pa	V1234	30 degree
13.00	0.031	19.50	Pab	V1234	30 degree
11.00	0.029	19.50	Pab	V1234	30 degree
11.00	0.029	19.50	Pab	V1234	30 degree
12.00	0.03	19.50	Pab	V1234	30 degree
12.00	0.03	19.50	Pab	V1234	30 degree
12.00	0.03	19.50	Pab	V1234	30 degree
12.00	0.03	19.50	Pab	V1234	30 degree
12.00	0.03	19.50	Pab	V1234	30 degree
12.00	0.03	19.50	Pab	V1234	30 degree
11.00	0.029	19.50	Pab	V1234	30 degree
17.00	0.037	19.50	Pt	V1234	30 degree
18.00	0.038	19.50	Pt	V1234	30 degree
18.00	0.038	19.50	Pt	V1234	30 degree
18.00	0.038	19.50	Pt	V1234	30 degree
18.00	0.038	19.50	Pt	V1234	30 degree
19.00	0.039	19.50	Pt	V1234	30 degree
18.00	0.038	19.50	Pt	V1234	30 degree
19.00	0.038	19.50	Pt	V1234	30 degree
18.00	0.038	19.50	Pt	V1234	30 degree
18.00	0.038	19.50	Pt	V1234	30 degree
8.00	0.025	20.20	Pa	V14	30 degree
6.00	0.022	20.20	Pa	V14	30 degree
5.00	0.02	20.20	Pa	V14	30 degree
7.00	0.023	20.20	Pa	V14	30 degree
5.00	0.019	20.20	Pa	V14	30 degree
5.00	0.02	20.20	Pa	V14	30 degree
5.00	0.02	20.20	Pa	V14	30 degree
7.00	0.023	20.20	Pa	V14	30 degree
6.00	0.021	20.20	Pa	V14	30 degree
6.00	0.021	20.20	Pa	V14	30 degree

Delta P (mbar)	Flow rate (l/s)	Mean T	Pressure	Voxers	Type
8.00	0.025	20.20	Pab	V14	30 degree
8.00	0.025	20.20	Pab	V14	30 degree
9.00	0.026	20.20	Pab	V14	30 degree
9.00	0.026	18.25	Pab	V14	30 degree
9.00	0.026	18.25	Pab	V14	30 degree
9.00	0.026	18.25	Pab	V14	30 degree
8.00	0.025	18.25	Pab	V14	30 degree
9.00	0.026	18.25	Pab	V14	30 degree
9.00	0.026	18.25	Pab	V14	30 degree
9.00	0.026	18.25	Pab	V14	30 degree
15.00	0.034	18.25	Pt	V14	30 degree
16.00	0.035	18.25	Pt	V14	30 degree
14.00	0.033	18.25	Pt	V14	30 degree
14.00	0.033	18.25	Pt	V14	30 degree
14.00	0.033	20.25	Pt	V14	30 degree
14.00	0.033	20.25	Pt	V14	30 degree
13.00	0.032	20.25	Pt	V14	30 degree
14.00	0.033	20.25	Pt	V14	30 degree
13.00	0.032	20.25	Pt	V14	30 degree
14.00	0.033	20.25	Pt	V14	30 degree
6.00	0.022	18.50	Pa	V14	30 degree 40 degree
8.00	0.025	18.50	Pa	V14	30 degree 40 degree
7.00	0.024	18.50	Pa	V14	30 degree 40 degree
8.00	0.025	18.50	Pa	V14	30 degree 40 degree
8.00	0.025	18.50	Pa	V14	30 degree 40 degree
8.00	0.025	18.50	Pa	V14	30 degree 40 degree
8.00	0.025	18.50	Pa	V14	30 degree 40 degree
8.00	0.025	18.50	Pa	V14	30 degree 40 degree
7.00	0.024	18.50	Pa	V14	30 degree 40 degree
8.00	0.025	18.50	Pa	V14	30 degree 40 degree
11.00	0.029	19.75	Pab	V14	30 degree 40 degree
11.00	0.029	19.75	Pab	V14	30 degree 40 degree
9.00	0.027	19.75	Pab	V14	30 degree 40 degree
9.00	0.026	19.75	Pab	V14	30 degree 40 degree
8.00	0.025	19.75	Pab	V14	30 degree 40 degree
8.00	0.025	19.75	Pab	V14	30 degree 40 degree
8.00	0.025	19.75	Pab	V14	30 degree 40 degree
9.00	0.026	19.75	Pab	V14	30 degree 40 degree
9.00	0.026	19.75	Pab	V14	30 degree 40 degree
9.00	0.026	19.75	Pab	V14	30 degree 40 degree

Delta P (mbar)	Flow rate (l/s)	Mean T	Pressure	Voxers	Type
23.00	0.042	19.75	Pt	V14	30 degree 40 degree
21.00	0.04	19.10	Pt	V14	30 degree 40 degree
22.00	0.041	19.10	Pt	V14	30 degree 40 degree
22.00	0.041	19.10	Pt	V14	30 degree 40 degree
23.00	0.042	19.10	Pt	V14	30 degree 40 degree
23.00	0.042	19.10	Pt	V14	30 degree 40 degree
21.00	0.041	19.10	Pt	V14	30 degree 40 degree
23.00	0.042	19.10	Pt	V14	30 degree 40 degree
23.00	0.042	19.10	Pt	V14	30 degree 40 degree
22.00	0.041	19.10	Pt	V14	30 degree 40 degree
7.00	0.024	20.75	Pa	V14	40 degree
9.00	0.026	20.75	Pa	V14	40 degree
9.00	0.026	20.75	Pa	V14	40 degree
9.00	0.026	20.75	Pa	V14	40 degree
8.00	0.025	20.75	Pa	V14	40 degree
9.00	0.026	20.75	Pa	V14	40 degree
9.00	0.026	20.75	Pa	V14	40 degree
9.00	0.026	20.75	Pa	V14	40 degree
8.00	0.025	20.75	Pa	V14	40 degree
9.00	0.026	20.75	Pa	V14	40 degree
9.00	0.026	20.75	Pab	V14	40 degree
10.00	0.027	19.70	Pab	V14	40 degree
9.00	0.026	19.70	Pab	V14	40 degree
10.00	0.027	19.70	Pab	V14	40 degree
10.00	0.027	19.70	Pab	V14	40 degree
10.00	0.027	19.70	Pab	V14	40 degree
9.00	0.026	19.70	Pab	V14	40 degree
10.00	0.027	19.70	Pab	V14	40 degree
10.00	0.027	19.70	Pab	V14	40 degree
9.00	0.026	19.70	Pab	V14	40 degree
18.00	0.037	19.60	Pt	V14	40 degree
24.00	0.043	19.60	Pt	V14	40 degree
24.00	0.043	19.60	Pt	V14	40 degree
24.00	0.043	19.60	Pt	V14	40 degree
23.00	0.042	19.60	Pt	V14	40 degree
24.00	0.043	19.60	Pt	V14	40 degree
22.00	0.041	19.60	Pt	V14	40 degree
24.00	0.043	19.60	Pt	V14	40 degree
23.00	0.042	19.60	Pt	V14	40 degree
24.00	0.043	19.60	Pt	V14	40 degree

## 5 Raw data from Keravan Energy test

Table 3: Guide for sorting the raw data chart

<b>Type</b>	$P_b$	$P_{ab}$
None	list1	list2
	list15	list17
	list16	list18
30 degree	list3	list4
	list6	list5
	list7	list9
	list8	list10
40 degree	list12	list11
	list13	list14

list1	list2	list3	list4	list5	list6	list7	list8	list9	list10	list11	list12	list13	list14	list15	list16	list17	list18
12	20	30	29	35	28	9	27	29	55	69	23	42	48	14	13	18	17
13	20	27	30	20	37	8	5	43	34	86	14	35	60	6	20	7	8
13	19	30	34	46	34	21	15	38	32	72	16	35	46	10	11	23	23
12	18	30	17	45	45	4	15	25	25	76	23	25	45	8	-5	1	17
13	19	28	19	36	35	12	15	32	30	74	17	12	45	14	42	6	25
12	19	27	30	42	44	2	16	36	36	61	17	19	55	-1	0	8	19
13	20	30	27	31	11	13	12	36	21	71	19	26	48	11	8	6	14
14	17	29	34	41	37	10	21	12	33	62	23	23	57	11	1	-6	19
11	19	30	11	44	44	5	6	34	26	59	19	6	53	13	27	9	15
10	20	29	14	37	33	3	22	45	37	76	8	22	60	11	-2	6	12
12	16	29	29	27	29	9	30	34	21	87	16	15	59	10	6	18	16
12	19	28	32	46	39	11	18	37	31	51	20	17	67	5	23	17	11
13	17	30	28	34	30	11	24	47	35	71	16	15	60	11	17	15	19
13	16	29	33	63	33	6	16	33	39	66	25	17	58	10	22	11	27
13	16	29	32	41	27	1	6	32	32	76	25	17	56	7	16	-9	11
13	17	29	-15	39	42	7	18	29	42	73	25	31	50	8	18	3	5
14	18	29	17	34	38	11	6	33	30	68	8	13	44	10	17	18	13
13	15	29	0	46	44	11	14	38	20	68	30	30	41	10	11	14	13
10	16	29	29	26	36	15	10	25	41	68	13	20	55	4	23	26	10
12	19	30	22	29	53	16	21	27	36	87	26	10	62	8	11	13	18
12	13	29	10	20	27	16	26	33	31	75	22	12	61	11	17	18	19
10	21	29	0	37	47	7	5	21	38	59	24	23	55	11	14	9	19
13	17	28	36	41	45	7	12	40	36	60	21	22	42	3	2	11	22
13	16	28	22	37	32	11	10	41	40	76	11	22	68	1	11	4	17
11	17	28	6	49	28	12	7	21	25	58	10	22	55	13	10	4	12
13	14	32	14	47	45	9	24	27	42	71	25	12	48	9	19	21	31
13	17	24	10	34	44	11	16	39	37	85	18	21	49	10	8	4	16
12	16	28	24	39	12	4	17	36	35	69	22	20	50	12	10	0	23
13	18	26	9	38	21	-1	17	43	32	61	6	19	52	9	3	17	22
11	19	26	33	38	31	10	7	43	42	85	15	18	59	12	14	3	22
11	19	27	21	33	28	6	18	31	39	74	18	18	58	12	21	7	17
13	18	25	10	41	20	12	11	37	39	70	20	24	58	1	8	3	7
13	16	27	0	39	36	6	14	46	29	66	5	24	46	14	11	15	26
12	19	27	18	31	40	13	15	26	23	76	22	21	47	5	23	35	11
11	14	28	30	28	36	8	8	51	34	64	24	18	46	6	10	14	32
12	16	30	13	18	44	17	12	24	29	64	15	9	51	3	19	22	21
15	18	30	30	40	35	7	21	43	28	59	28	17	45	7	31	9	15



list1	list2	list3	list4	list5	list6	list7	list8	list9	list10	list11	list12	list13	list14	list15	list16	list17	list18
11	18	30	16	37	29	9	16	45	30	61	19	13	67	12	17	13	18
13	21	29	28	25	39	7	10	37	22	74	28	24	56	9	18	19	4
12	21	27	20	32	44	14	22	33	37	79	29	21	64	7	16	11	19
11	21	27	19	49	39	5	20	46	29	72	16	26	53	11	15	15	13
11	18	30	11	36	39	7	14	58	21	80	19	27	57	8	-4	10	18
12	19	29	15	29	39	12	9	40	25	53	14	27	44	10	22	-2	18
12	19	28	18	40	34	6	17	23	26	76	12	18	47	10	10	9	14
12	15	22	24	30	28	10	23	33	38	61	20	28	59	8	7	19	10
12	17	33	14	45	22	20	18	36	44	69	17	23	58	2	4	3	15
11	16	26	27	37	54	16	14	26	33	78	32	27	61	13	15	-5	21
11	20	27	21	43	35	4	23	15	25	80	22	9	51	10	3	13	0
13	21	28	-2	26	27	13	13	19	35	78	6	13	61	11	-4	14	14
12	18	26	34	46	25	14	18	47	35	77	16	21	52	16	20	10	22
13	16	31	29	34	40	15	23	24	25	73	13	12	51	7	7	10	14
14	19	29	15	52	40	5	19	36	34	75	29	20	60	7	0	10	27
15	17	30	18	21	35	4	17	38	36	78	16	37	56	14	19	-6	22
12	19	27	4	35	30	8	13	38	40	65	20	13	49	11	15	9	13
13	20	26	17	41	36	21	35	28	37	62	18	21	51	13	16	-9	12
13	20	27	31	15	38	-1	14	23	45	72	18	22	46	6	18	-1	8
12	21	27	22	24	40	8	4	35	42	90	28	26	52	10	21	1	17
10	16	27	-1	18	28	6	26	47	31	77	21	31	58	2	1	2	8
11	17	25	16	25	26	13	16	45	23	72	32	9	46	6	2	9	24
12	12	29	9	27	49	11	5	37	28	81	16	27	59	6	5	8	17
11	17	30	32	47	36	7	15	41	26	78	13	23	52	8	-2	18	12
12	16	30	30	38	38	12	19	29	15	62	14	25	54	11	19	9	4
13	18	27	31	39	36	10	15	31	36	68	14	20	45	2	-8	10	13
12	18	27	19	18	42	5	24	26	46	78	15	30	64	11	2	10	11
12	20	28	9	29	44	6	8	33	29	61	20	18	55	10	4	14	21
10	19	27	16	37	39	16	8	36	31	88	32	15	53	17	21	6	22
13	16	26	34	40	38	7	22	14	35	71	27	18	64	14	18	-4	18
14	17	27	17	43	35	3	9	29	28	78	22	19	55	15	14	11	19
13	22	27	37	33	37	3	14	29	35	64	20	3	42	8	20	16	13
12	14	29	12	26	32	2	20	41	39	76	26	22	57	10	14	7	24
12	16	28	27	15	37	17	14	32	36	61	12	16	48	11	11	4	22
11	19	29	10	35	34	0	12	45	37	72	20	23	62	15	32	5	22
12	19	25	7	46	21	2	22	50	21	77	13	25	54	5	7	12	29

list1	list2	list3	list4	list5	list6	list7	list8	list9	list10	list11	list12	list13	list14	list15	list16	list17	list18
13	16	25	27	55	33	15	6	20	34	60	25	18	59	5	15	10	11
11	22	27	60	40	40	8	5	25	41	79	7	30	49	14	18	15	14
11	18	28	25	42	39	25	17	39	39	66	19	21	46	13	2	11	5
11	21	27	-8	44	35	23	11	51	30	73	17	27	58	2	23	-8	26
12	17	28	20	36	35	10	36	37	22	80	23	23	57	7	34	0	14
11	22	30	24	27	41	7	14	44	38	75	22	35	58	6	21	11	20
10	19	29	22	19	30	16	7	32	42	71	21	21	55	16	1	5	9
11	14	27	4	37	41	9	14	24	39	79	13	13	48	12	25	9	24
11	18	26	19	38	34	14	16	42	25	74	19	23	52	12	18	3	9
11	17	27	21	30	30	6	27	28	50	70	11	31	57	8	10	10	14
13	19	28	19	45	28	9	14	30	33	52	24	29	59	7	1	9	24
11	19	30	36	32	28	12	18	17	49	76	20	25	54	19	14	8	18
12	18	31	34	32	31	7	12	29	44	65	15	14	51	10	20	3	12
14	20	34	6	36	30	4	12	38	20	62	34	3	57	2	-7	10	17
10	15	30	40	39	23	5	17	18	18	69	34	28	45	9	12	16	19
14	17	29	8	23	40	21	17	32	34	66	20	28	51	2	12	9	28
10	15	29	24	52	43	11	25	23	34	63	21	14	40	11	12	20	22
11	21	29	6	28	28	10	22	31	36	50	1	28	61	8	13	13	12
14	21	26	-1	30	46	6	18	36	32	69	33	29	56	11	10	21	8
12	16	30	11	21	31	6	12	35	35	82	12	7	60	14	13	17	12
13	19	27	4	24	32	14	12	46	25	77	27	38	65	15	-7	20	14
12	22	25	5	50	34	5	19	29	38	65	21	23	59	12	3	-5	14
12	17	29	26	35	26	26	18	34	31	81	23	14	59	8	19	-6	5
14	21	27	19	34	45	-1	11	23	42	48	23	25	62	2	17	11	26
12	19	30	33	44	46	13	12	23	11	70	17	34	51	13	4	4	14
12	19	30	34	37	29	0	13	37	39	82	25	6	56	5	19	4	22
12	18	27	12	53	37	4	21	25	41	68	19	23	52	7	-6	5	13